Microwave Journal E-BOOK

GaN Power Amplifier Design Solutions

SEPTEMBER 2018

SPONSORED BY Boonton qorvo

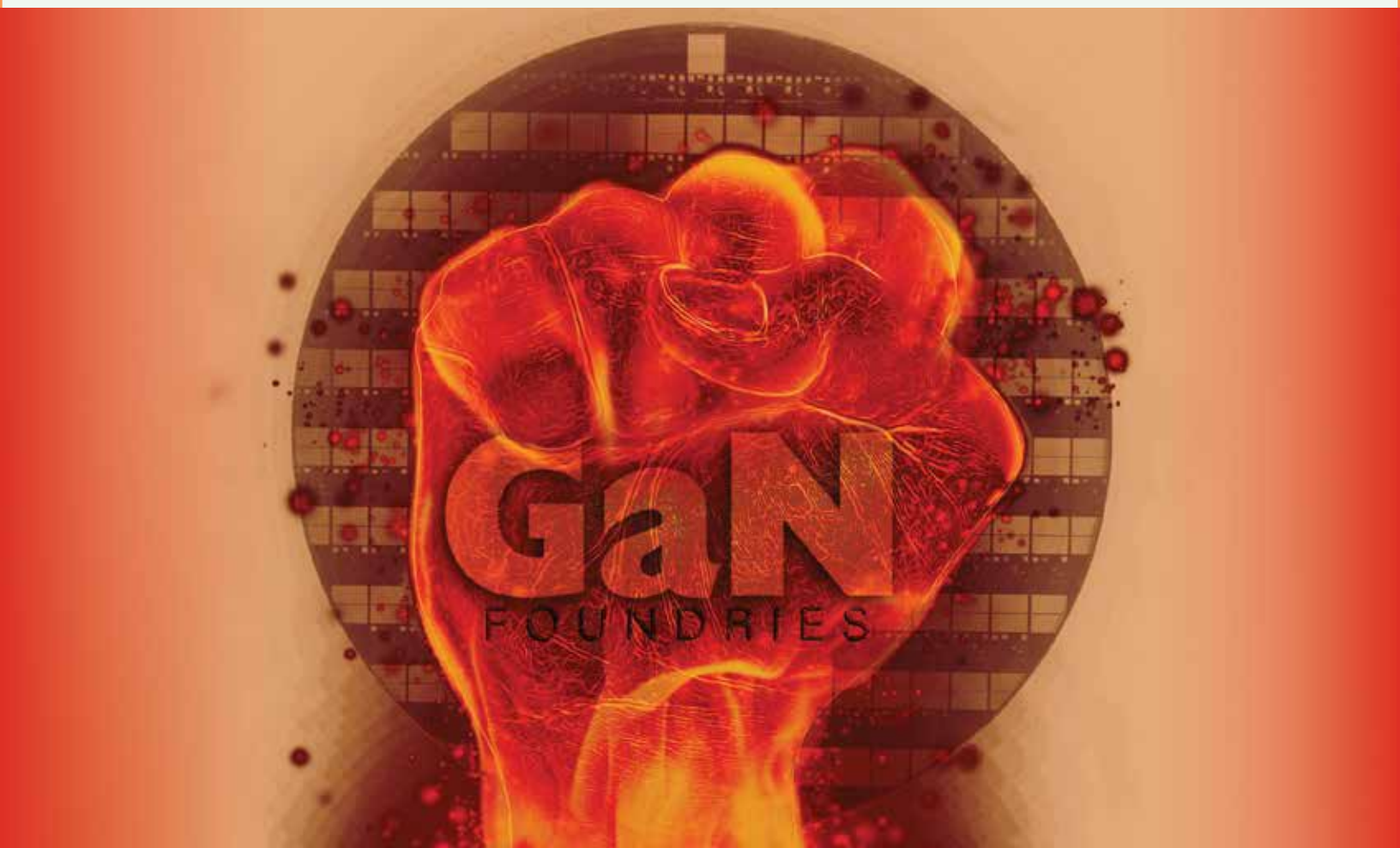

Table of Contents

Introduction

GaN Power Amplifier Design Solutions

According to Strategy Analytics, the RF GaN market growth continued to accelerate in 2017, with revenue growing at over 38 percent year-on-year. With GaN seeing adoption across a variety of RF applications, the rollout of commercial wireless infrastructure coupled with demand from military radar, electronic warfare and communications applications are providing the primary drivers for growth. They forecast that RF GaN revenues will exceed $1 billion by the end of 2022, with defense sector demand slightly greater than commercial revenue.

Strategy Analytics reported that RF GaN demand from the military sector grew by 72 percent year-on-year in 2017, and they project it will grow at a compound annual average growth rate of 22 percent through 2022. The military radar segment remains the largest user of GaN devices for the defense sector, with substantial production activity in AESA radars for land-based and naval systems being the main driver for increasing demand of RF GaN.

They also note that wireless base stations continue to be the largest revenue segment for RF GaN, with increasing market penetration resulting in year-on-year growth of more than 20 percent. While the big lift from Chinese LTE deployments is over, the wireless industry has maintained and, in some cases, compressed the 5G deployment schedule. The resulting 5G base station deployment will become a primary commercial growth driver for RF GaN.

With RF GaN amplifier activity continuing to increase, this eBook provides six articles covering various design topics in commercial and military markets. The first two stories cover Aerospace & Defense applications with GaN being used in the Space Fence Radar System and as replacements for TWTAs in ECM systems. The next article takes a look at the adoption of GaN in the point to point microwave radio systems authored by Ericsson. With the high power densities achieved by GaN amplifiers, the thermal challenges can even be more critical than the electronic design issues so the next three articles look at addressing thermal challenges through heat sinking/mechanical design and various design techniques and solution to improve efficiency. We hope that this will improve your knowledge of GaN amplifier technology and thank Boonton and Qorvo for sponsoring this eBook.

Pat Hindle, Microwave Journal Editor

Space Fence Radar Leverages Power of GaN

Justin Gallagher, Joseph A. Haimerl, Thomas Higgins and Matthew Gruber
Lockheed Martin MST, Moorestown, N.J.

Editor's Note: Because of its high power density, GaN is widely recognized as providing a step-function increase in the capability of solid-state power amplifiers. Arguably not as well known is the impact GaN is having at the system level, particularly military systems. While logical to assume GaN enables evolutionary improvements, in some cases the system would not be possible without GaN. The Space Fence radar is one example, described in this article by Lockheed Martin.

GaN is a compound semiconductor using III/V group elements that represents a leap ahead of existing GaAs technologies for many RF applications. GaN high electron mobility transistors (HEMT) are constructed using very similar fabrication techniques as GaAs RF devices but provide significant advantages.

The reason for the leap in technology GaN has over GaAs results from significantly higher operating RF power density and higher reliability. The secondary benefits built on these first two are: smaller chips for a given output power; smaller modules; higher overall efficiency due to lower combining losses; lower module assembly cost; higher power handling survivability and higher impedance for large devices, making for easier impedance matching.

The inherent advantage of GaN over GaAs is due to basic physics of the devices and materials. GaN is referred to as a wide bandgap semiconductor because of the wider energy gap between the valence and conduction bands, compared to conventional semiconductors. The wider energy gap (3.4 eV for GaN compared to 1.42 eV for GaAs) allows higher electric field strengths and higher breakdown fields, which translate into higher operating voltages.[1]

Another advantageous characteristic of GaN is electron drift velocity, which in GaN increases with higher field strength, while it decreases with higher field strength in GaAs. Another way of describing it is that the low field drift velocity of GaAs is superior to GaN, but the high field drift velocity of GaN is far superior to GaAs. The peak in this characteristic (electron drift velocity vs. field strength) is the saturation velocity. In GaN it is 2.46 × 107 cm/s, while GaAs is 1.8 × 107. However, at high fields where GaN is 2.46 × 107, GaAs electron drift velocity is under 1 × 107.1 Since electron drift velocity is related to current density, it basically means that at high voltage, GaN is also capable of high current, whereas GaAs is not. Also, since power is a function of voltage and current, the wide energy gap and high drift velocity make for ideal high power devices. For these reasons, GaAs will never outperform GaN for high power applications; however GaAs should retain its applicability in low voltage and low power applications.

A third important aspect of GaN technology, especially for power devices, is the substrate

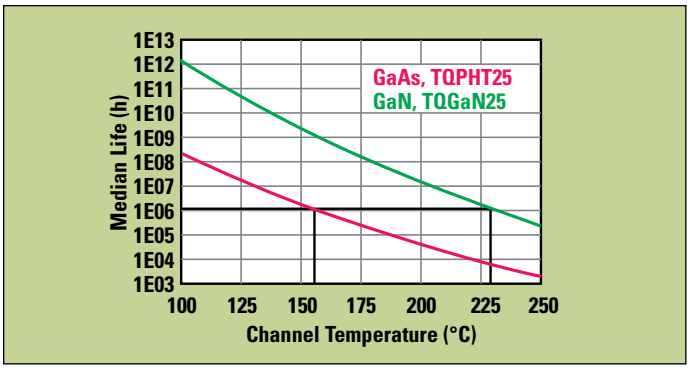

Fig. 1 Reliability comparison of Qorvo GaN and GaAs PHEMT processes.

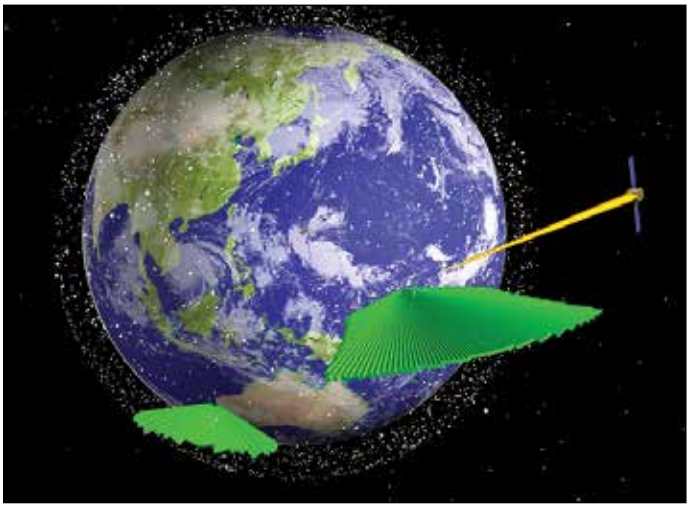

Fig. 2 Space Fence comprises two radars, one located near the equator at Kwajalein Atoll and an optional second site in Western Australia.

material. Since GaN substrates were not very advanced and were thermally inferior, silicon carbide (SiC) emerged as the best substrate material for GaN RF power devices. The thermal conductivity of SiC is superior to other substrates, such as silicon or sapphire, and allows the high power potential of GaN to be realized. The thermal conductivity of SiC is approximately 10× better than GaAs. These advantages allow operation of systems and sensors that would not have been possible with GaAs semiconductors. For example, new systems have steep requirements for both performance and operational availability. GaN enables sensors to operate with longer reliability and be driven harder (i.e., longer pulse width per duty cycle), based on the inherent higher power density properties.

Assessing reliability, GaN devices can operate at a much higher channel temperature than GaAs for equivalent reliability; at equivalent channel temperatures, GaN achieves much higher reliability. Comparing the reliability of Qorvo's GaN and GaAs technologies (see ***Figure 1***), at Tc = 150°C the median life of GaN is 1 × 109 hours vs. 1 × 106 hours for GaAs. At 1 × 106 hour median life, GaN can operate 75°C hotter than GaAs (i.e., 225°C for GaN vs. 150°C for GaAs).[2]

Overall, GaN can lead to smaller, cheaper, more efficient and higher power RF modules. For example, a single GaN MMIC high power amplifier (HPA) can replace a pair of GaAs HPAs which need a power combiner/divider, extra supporting components and additional assembly. Efficiency is gained not only at the MMIC level, where on-chip combining losses are reduced, but also at the module level, where combining losses are eliminated when two or more GaAs HPAs need to be combined.

Use of GaN HPAs in solid-state phased array radar provide numerous benefits. As described, GaN supports higher output power, higher transmit duty factor and longer pulse lengths than previous technologies, such as GaAs and Si BJT. These allow smaller aperture sizes and reduce overall system acquisition costs. Since GaN operates at higher efficiency, operational costs are also reduced, as less prime power is consumed and less heat is dissipated, reducing the need for active cooling. An example of this would be an existing radar which utilizes a solid-state semiconductor such as GaAs. An equally sized radar employing GaN would benefit from a significant increase in radar range with a slight increase in prime power. Conversely, for the same prime power, the power density of GaN could significantly reduce the radar aperture. This has first order effects of reducing acquisition costs, including both front-end and back-end electronics. Lastly, GaN has higher reliability than previous technologies. Higher reliability reduces operational costs through reduced maintenance and spare parts.

SPACE FENCE RADAR

Space Fence is a ground-based system of S-Band radars designed to greatly enhance the U.S. Air Force Space Surveillance Network. Space Fence provides unprecedented sensitivity, coverage and tracking accuracy and contributes to key space mission threads, with the ability to detect, track and catalog small objects in low Earth orbit (LEO), medium Earth orbit (MEO) and geosynchronous orbit (GEO). Space Fence's capabilities of detecting, tracking and cataloging hundreds of thousands of satellites and debris in orbit around the earth will revolutionize space situational awareness.[3]

Space Fence includes up to two minimally manned radar sites (see ***Figure 2***). The first radar site is under construction on Kwajalein Atoll in the Pacific Ocean near the equator and is expected to become operational in late 2018. The second site, currently an unfunded contract option, is located in Western Australia. The sensor sites provide assured coverage for objects in LEO and are integrated through an operations center located in Huntsville, Ala.

The initial Kwajalein radar will provide a persistent surveillance "fence" comprised of thousands of radar beams covering LEO altitudes. As the Earth rotates, this fence sweeps the space around the Earth, providing assured coverage to detect satellites and orbital debris. To form high quality orbital estimates, objects that cross the fence are tracked over long arcs with dedicated beams. Space Fence can also be tasked to search for higher altitude objects in MEO and GEO. The optional second site will complement the first site's LEO coverage and also provide tasking capability to MEO and GEO.[3]

As shown in ***Figure 3a,*** each radar site features a design with closely spaced but separate transmit and receive phased array antennas, prime power and liquid cooling. The transmit array building houses a 36,000 element transmit phased array antenna beneath an air supported low loss Kevlar environmental radome. The receive building supports an 86,000 element array, also under a low loss

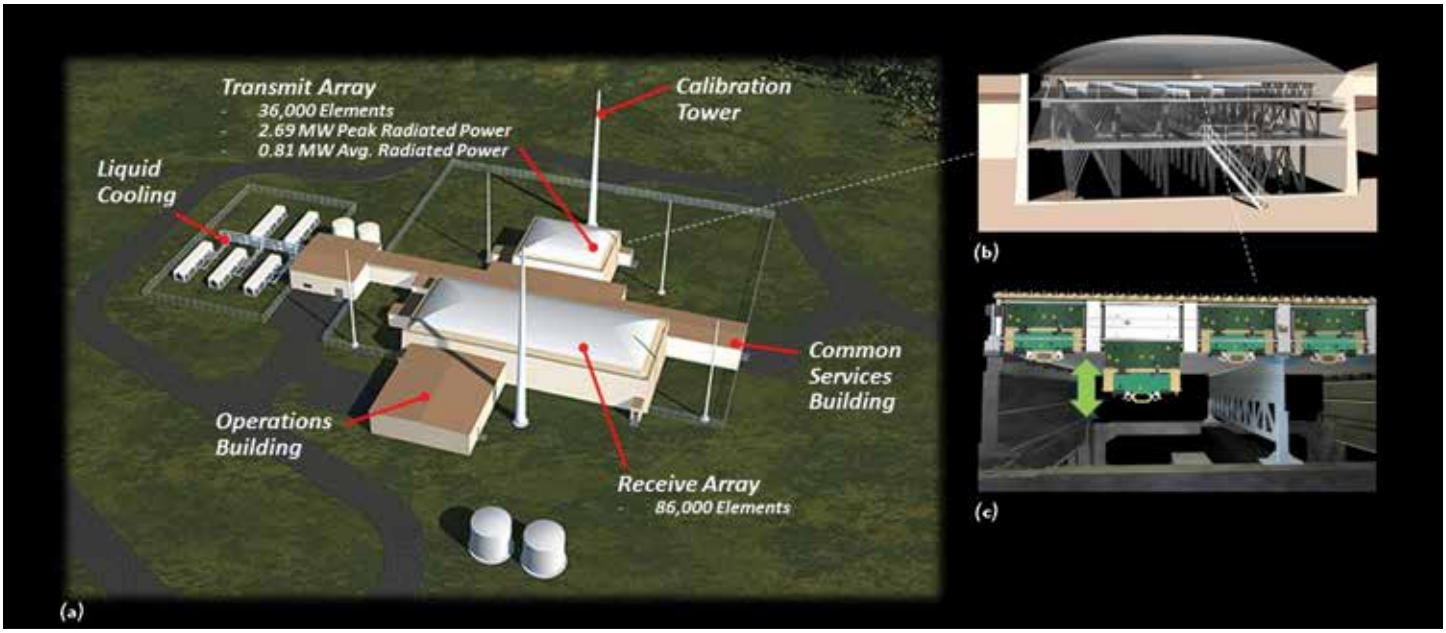

▲ Fig. 3 Space Fence radar site (a) cutaway of the transmit array (b) and cross-section of the "radar-on-a-board" transmit LRUs (c).

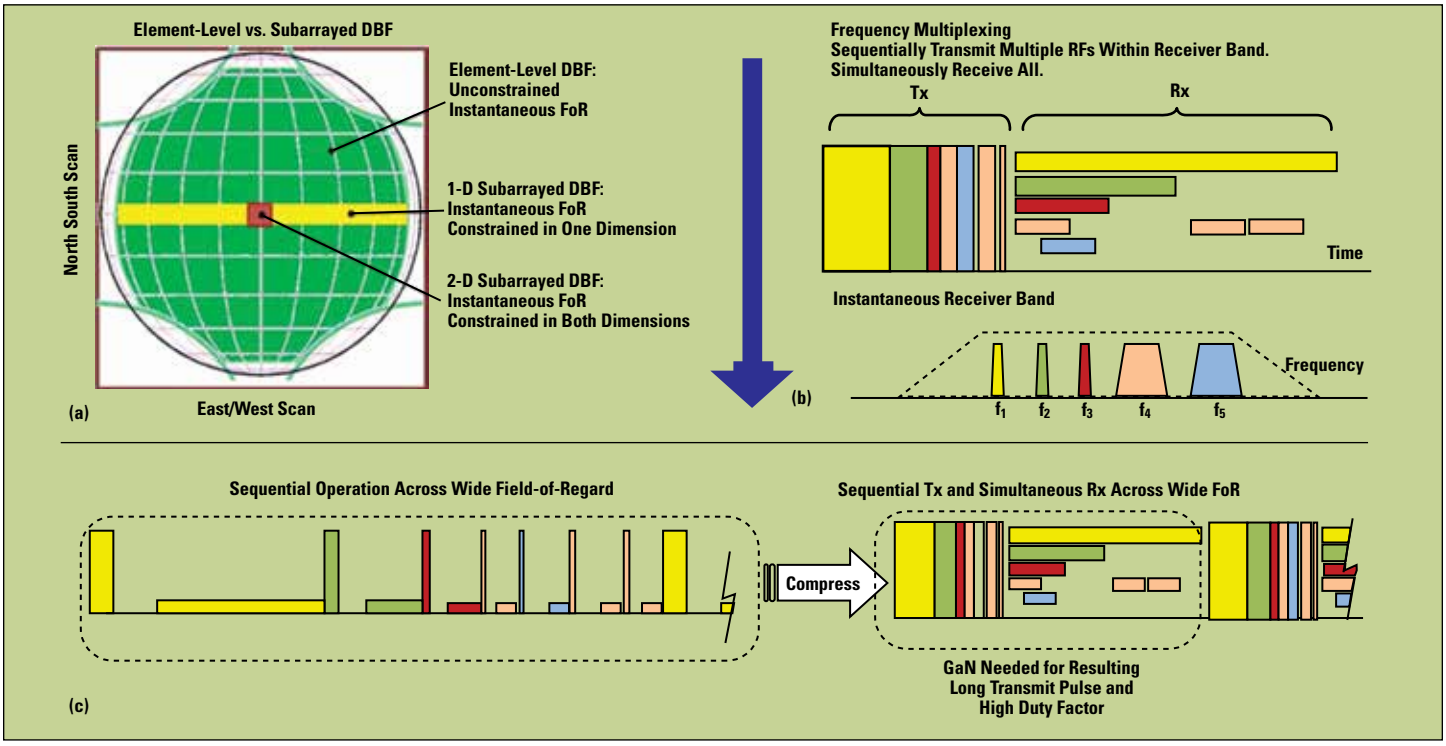

▲ Fig. 4 Digitizing at the element, instead of combining multiple elements into subarrayed receivers, enables beams to be formed anywhere in the array FoR (a). Multiple frequency channels, each for a different radar function, can be received at the same time by beams on the receive array, allowing many functions to be performed simultaneously (b). GaN is the only technology that supports the "machine gun" transmit sequence, with long pulses and high duty factor (c).

Kevlar radome. Both arrays are provided power and cooling through the common services building. Radar data processing and control of the apertures is performed off-array in commercial off-the-shelf (COTS) processing equipment located within the operations building. Both transmit and receive arrays are automatically calibrated with horns that are mounted on calibration towers and can transmit or receive test signals. The extremely large phased arrays are optimized for high availability and low lifetime support costs and use GaN HPAs for transmit amplification, providing unprecedented sensitivity to detect small objects. On receive, digital beam forming (DBF) at the element level permits thousands of simultaneous beams instantaneously in any direction. This enables the system to provide persistent LEO surveillance coverage while simultaneously tracking hundreds of objects, performing cued search tasks in other surveillance regimes (including MEO and GEO) and supporting user-defined flexible surveillance volumes. Transmit and receive arrays are oriented to face straight up and are designed integrally with the building (see the transmit array cutaway in Figure 3b). A scalable facility structure supports liquid cooled cold plates, which house the radar electronics. Radiator tiles are mounted on the top of the cold plates while "radar-on-a-board" digital transmit and receive line replaceable units (LRU) are mounted on the sides ***(Figure 3c).*** Each transmit LRU incorporates digital waveform gen-

(a)

(b)

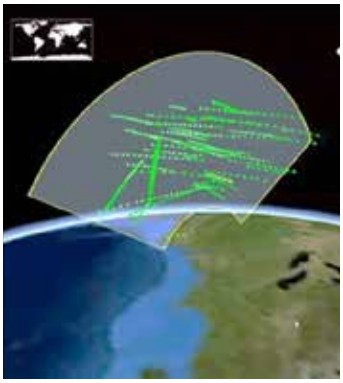

(c)

▲ **Fig. 5 Space Fence prototype: antenna building (a) mission operations center (b) and critical design review (CDR) demonstration.**

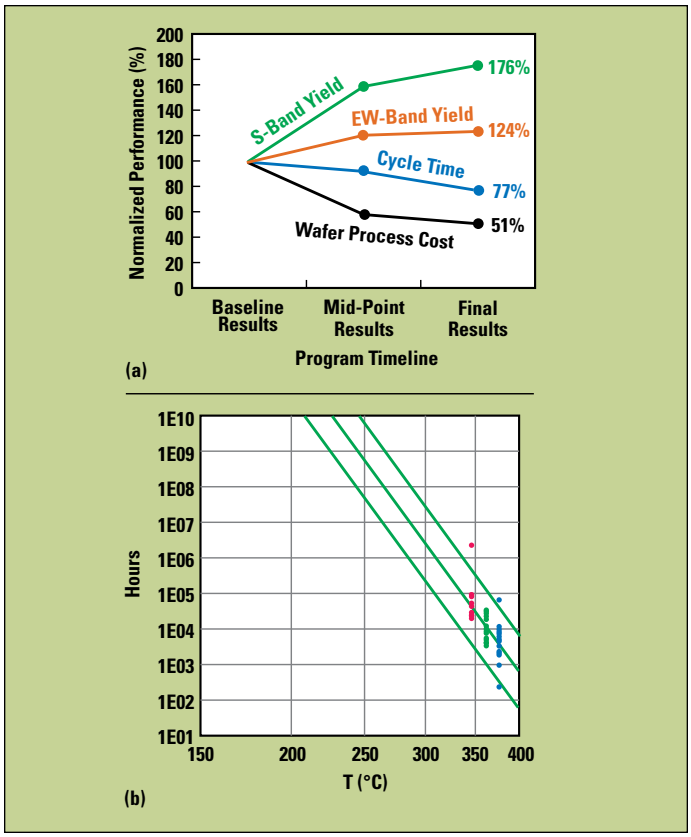

▲ **Fig. 6 Wolfspeed DPA Title III performance improvement (a) and reliability (b).**

eration, up-conversion to S-Band and high power GaN amplification for eight transmit radiating elements. Mounting the LRUs on the sides of the cold plates provides the GaN HPAs with a direct and efficient thermal path. To provide high system availability, the LRUs are serviceable from beneath the array and can be removed and replaced in less than 1½ minutes while the array is operating.

GaN high power amplification was one of the critical enabling technologies for the Space Fence solution. Relative to other technologies, the high output power of GaN reduces the number of transmit elements to achieve the required sensitivity for the target size, which reduces overall acquisition cost. GaN's high efficiency also reduces power consumption and heat dissipated, which reduces operational costs for the sensor site. In order to effectively support the LEO orbital regime (and tasking up to GEO) and get sufficient energy back for detection, transmit pulse lengths need to be long. Previous technologies, such as GaAs or Si BJT didn't support these pulse lengths at the required output power.

The long pulse capability of GaN in the transmit array also enables extremely efficient timeline utilization of the radar when combined with element level DBF in the receive array. Space Fence has a receiver connected to each array element within the receive array to digitize the returned signals. Unlike subarrayed antennas, which combine multiple elements in microwave electronics prior to digitizing to reduce the number of receivers, the beams in an element level DBF system can be simultaneously placed anywhere in the field-of-regard (FoR) of the array. Subarrayed approaches limit the digitally formed beams to constrained volumes and require changing analog phase shifters to move the volume from one radar event to the next ***(Figure 4a).*** Space Fence is able to use its flexibility along with frequency multiplexed functions within the receiver band to form thousands of beams simultaneously ***(Figure 4b).*** This allows many functions that would have been performed sequentially to be performed simultaneously, reducing the Space Fence array sizes along with the associated acquisition cost and operating costs. Use of GaN HPAs are needed to support the resulting concatenated "machine gun" like transmit sequence, which is longer and transmit higher duty factor than supported by other technologies ***(Figure 4c).***

At the start of concept development for Space Fence in 2007, Lockheed Martin leveraged an existing Independent Research and Development (IRAD) project that was maturing GaN for use in radar applications. Over the course of the Space Fence development, GaN was optimized to the Space Fence application for additional efficiency and reduced operational costs. Lockheed Martin also embraced an open foundry concept and worked with two suppliers to develop GaN for Space Fence. Space Fence transmit LRUs have been successfully tested with GaN modules from both of these companies. Use of multiple suppliers reduced program risk and provided competition to reduce acquisition costs.

With the large Space Fence arrays and number of GaN devices, high reliability is necessary to keep maintenance costs down. To ensure mature technology, Lockheed Martin tested the Space Fence GaN amplifiers at the module, at

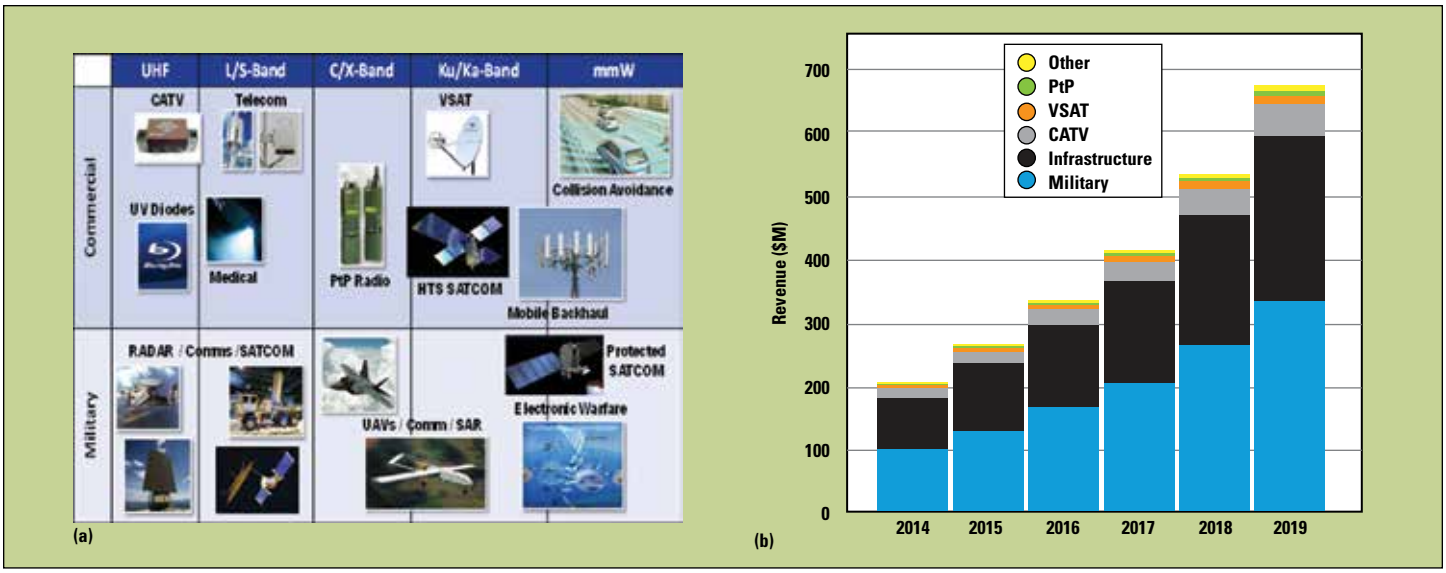

▲ **Fig. 7 Commercial and military products using GaN (a) and projected GaN market growth (b). Commercial pull for GaN will be more than 2x military applications by 2019.[6]**

the transmit LRU and at the array. After years of extensive testing (more than 5,000 hours of life testing, including accelerated life testing), the technology has proven to be extremely robust, showing a high reliability confidence level which supports the rigorous operational availability of the mission.

Since 2011, Lockheed Martin has had an operational end-to-end system prototype employing all its critical technologies, including GaN and element level DBF, in scaled-down arrays (see ***Figure 5***). Prototype system data was used by the U.S. Air Force in a technology readiness assessment in 2015, resulting in a Technology Readiness Level (TRL) 7 and Manufacturing Readiness Level (MRL) 7. In January 2016, an Integration Test Bed (ITB) using final production hardware was commissioned in Moorestown, N. J. The ITB supports hardware/software integration, maintenance training and verification testing; it will provide remote support to the integration of Sensor Site 1 on Kwajalein Atoll.

OPEN FOUNDRY MODEL

The development of GaN with ever increasing government funding has been occurring since the 1970s.[4] Since the early 2000s, both the Department of Defense and commercial foundries have considerably increased this funding. One example is the DARPA Wide Bandgap program which funded various semiconductor foundries to mature the technology, investing approximately $150 million. This program followed the successful initiatives of the 1980s and 1990s to fund GaAs, such as DARPA's MIMIC and MAFET programs. Among the key parameters and facets of the technology development were the physics of the devices, to understand and unleash the potential of the superior physical properties of the semiconductors, and the development of accurate models.

The completion of the DARPA Wide Bandgap program in 2011 led to an additional program funded through the Defense Production Act (DPA) Title III program office. The mission of the DPA Title III program is to "create assured, affordable and commercially viable production capabilities and capacities for items essential for national defense." The main focus of the GaN Title III program was to improve the manufacturability of GaN, essentially to increase the MRL to level 8. The program was structured as three phases: 1) baseline manufacturing readiness, 2) improvement and refinement of processes and 3) final manufacturing readiness assessment.

TABLE 1

GAN MARKET SHARE STRATEGY ANALYTICS, JANUARY 2015

	Military Segment	*Total Worldwide*
Wolfspeed	19%	25%
Qorvo	24%	22%
Sumitomo	17%	22%
Raytheon	13%	7%
Northrop Grumman	11%	6%
UMS	6%	6%
Others	10%	12%

Wolfspeed was able to substantially increase their yield over the three phases, while simultaneously reducing cycle time and wafer processing costs (see ***Figure 6***).[5] Over the three phases, yield increased 76 percent for S-Band devices, cycle time reduced 23 percent and wafer costs decreased 49 percent. Reliability of 1 × 107 hours was demonstrated at a channel temperature of approximately 275°C. Through manufacturing process refinement and building significant robust wafer lots, Wolfspeed reached MRL 8 in 2014, i.e., demonstrated pilot line capability and ready to begin low rate initial production (LRIP). One of the other major commercial foundries, Qorvo (formerly TriQuint) was the only funded foundry that achieved MRL 9 in 2014, i.e., demonstrated LRIP and capability in place to begin full rate production (FRP).

GaN has been inserted into several Lockheed Martin and other DoD contractor systems and has achieved TRLs through level 9. Space Fence has achieved TRL 7. Since the

completion of both the DARPA Wide Bandgap and DPA Title III programs, GaN has been following a Si CMOS trajectory, in terms of applications and utilization in commercial markets.6 GaN has found its way into base stations, medical equipment and even residential/commercial lighting available at local hardware stores (see ***Figure 7***).

Lockheed Martin employs an open foundry model (LM OpenGaN), which leverages the commercial market for the best technology at the most competitive cost. The cost of owning and running a foundry year after year can be significant. Given the growth projections for semiconductors, in general, it makes more sense to allow high commercial volumes to mature the technology process and drive costs down.7 A study conducted by Strategy Analytics[6] (see ***Table 1***), identified Qorvo and Wolfspeed as GaN leaders, with no other domestic suppliers close to providing equivalent volume. In the semiconductor industry, volume production lends itself to higher maturity, stable processes and lower costs.

Lockheed Martin adopted an open foundry model to address the Department of Defense's official memorandum on Better Buying Power 3.0 and the "3rd Offset," with the goal of increasing the capability and rapid technology development required by the warfighter.[8] It is not economical to have any particular foundry develop various semiconductor processes, not just III/IV (i.e., GaAs, GaN, InP) but also SiGe and CMOS.

GaN has had significant investment over the past 10 years and is proven to be field ready, reliable and cost competitive with existing technologies (e.g., GaAs). The system benefits enable enhanced capabilities for backfit military systems and are required for the performance of future systems. The Space Fence program would not have been possible without GaN nor as successful without the affordability enabled by the LM Open GaN foundry model.

THE FUTURE

The next generation of GaN development is focused around increasing capability by pushing into higher operating frequencies, improving thermal performance and enabling chip-scale integration of GaN with other IC technologies. Developments of 150 nm and 90 nm process nodes will extend ft to 60 and 100 GHz, respectively.

While DBF systems such as Space Fence represent a significant capability upgrade, the challenges from the increased IC design complexity in the areas of size, weight and power (SWAP), bandwidth and latency performance must be overcome. To address this, programs such as DARPA's Diverse Accessible Heterogeneous Integration (DAHI) program are focused on developing chip-scale integration of GaN with high density Si CMOS, as well as other technologies such as InP and MEMS. These resulting capabilities will enable the wider proliferation of the high performance mixed-signal integration solutions required to develop the capabilities to further advance state-of-the-art sensor systems.

While GaN is capable of generating extremely high RF power densities, thermal management remains a significant challenge, especially at higher frequencies where thermal density is most extreme. On the DARPA IceCool program, Lockheed Martin has made tremendous gains in unlocking the ultimate potential of millimeter wave GaN by developing a micro-fluidically cooled HPA with a 3×reduction in thermal resistance compared to conventional thermal management solutions. This IceCool solution enables an 8.3 dB increase in output power for the same device, while simultaneously reducing operating temperature by increasing power-added efficiency between 2.5× and 3.5×.[9] Overall, these advancements will further extend the true potential of GaN and its ability to realize tremendous capability upgrades for a wide variety of systems. ■

ACKNOWLEDGMENT

The authors would like to acknowledge and thank the Space Fence and ICECool sponsors (AFLCMC, DARPA and AFRL) and partners for their financial and technical support.

References

1. Liou Schwierz, "Modern Microwave Transistors," *Wiley,* 2003.
2. R. Hall, "GaN at Qorvo" *Presentation,* August 2015.
3. Joseph A. Haimerl and Gregory P. Fonder, "Space Fence System Overview," *Advanced Maui Optical and Space Surveillance Technologies Conference Proceedings,* September 2015.
4. M. Yoder, "Gallium Nitride Past, Present, and Future," *IEEE/Cornell Conference on Advanced Concepts,* 1997.
5. Ryan Fury, Scott T. Sheppard, Jeffrey B. Barner, Bill Pribble, Jeremy Fisher, Donald A. Gajewski, Fabian Radulescu, Helmut Hagleitner, Dan Namishia, Zoltan Ring, Jennifer Gao, Sangmin Lee, Brian Fetzer, Rick McFarland, Jim Milligan and John Palmour, "GaN on SiC MMIC Production for S-Band and EW-Band Applications," *CS ManTech Conference,* May 13–16, 2013, New Orleans, La.
6. Eric Higham, Strategy Analytics, "An Overview of GaN RF Device Market," *GaN Roundtable Session,* August 26, 2015.
7. Justin Gallagher, "The Commercialization of GaN," *Defense Manufacturing Conference Proceedings,* November 2015.
8. Under Secretary of Defense, "Implementation Directive for Better Buying Power 3.0 – Achieving Dominant Capabilities through Technical Excellence and Innovation," Memorandum, 2015 http://bbp.dau.mil/docs/BBP3.0ImplementationGuidanceMemorandumforRelease.pdf.
9. J. Ditri, R. Cadotte, D. Fetterolf and M. McNulty, "Impact of Microfluidic Cooling on High Power Amplifier RF Performance," *Proceedings of the 15th Intersociety Conference on Thermal and Thermomechanical Phenomena in Electronic Systems (ITHERM 2016),* Las Vegas, Nev., 2016.

Solid-State PAs Battle TWTAs for ECM Systems

Rick Montgomery and Patrick Courtney
Qorvo, Greensboro, N.C.

Electronic countermeasures or ECM systems are typically comprised of receivers, processors, displays and jamming transmitters. Until recently, solid-state amplifiers fell short of the required combination of power, bandwidth and efficiency for the transmitter of an ECM system. Maturating GaN power amplifier MMICs and low loss, broadband combining techniques now make it possible to meet the power, bandwidth and efficiency requirements of ECM systems with solid-state power amplifiers (SSPA). Compared to GaAs and other solid-state semiconductor materials, GaN provides an order-of-magnitude increase in transistor power density, and the higher impedance of the devices eases the design of matching networks.

Historically, traveling wave tubes (TWT) and other vacuum tubes have provided the microwave power for ECM transmitters. Since the 1950s, the broadband, high-power microwave amplification necessary for ECM transmitters was only feasible with vacuum tube technology and, in particular, with traveling wave tube amplifiers (TWTA). ECM jamming transmitters typically need to generate hundreds of watts of microwave power over several octaves. The efficiency of the amplifiers must be high enough to meet the limited power budget of airborne platforms and the heat generated can be dissipated. TWTAs were the only technology that could meet these critical requirements.

SOLID-STATE VS. TUBE

Solid-state devices have long been preferred to vacuum devices. Vacuum tubes, with their associated high voltage power supplies—typically in the multi-kV range—have lower reliability than solid-state devices operating with low voltage power supplies (i.e., under 50 V). Manufacturers and users of vacuum tubes face diminishing sources of supply and material shortages.

Solid-state devices generate lower noise and have better linearity than vacuum tubes. For instance, solid-state devices in "standby mode"—where the DC bias voltage is applied with no RF input signal—generate significantly less noise power across the spectrum. Noise figures for a medium power TWT can be around 30 dB, versus about 10 dB for a solid-state GaN MMIC PA. This is a significant difference in an ECM system, as the lower noise may allow the transmitter's output stage to remain in standby mode when not transmitting. The overall switching time decreases, since the main DC power to the PA does not need to be switched on and off.

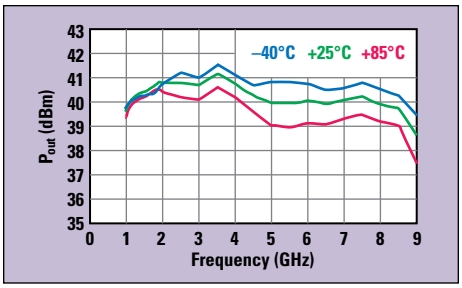

▲ **Fig. 1 Output power vs. frequency and temperature of a Qorvo QPA1003P GaN MMIC, with 15 dBm CW input power, 28 V bias and 650 mA current consumption.**

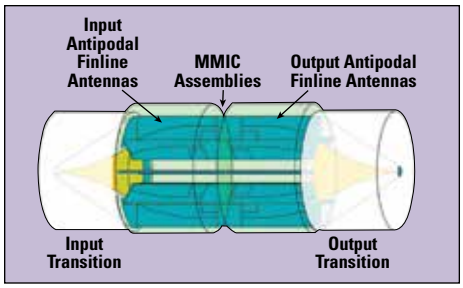

▲ **Fig. 2 Spatium amplifier structure.**

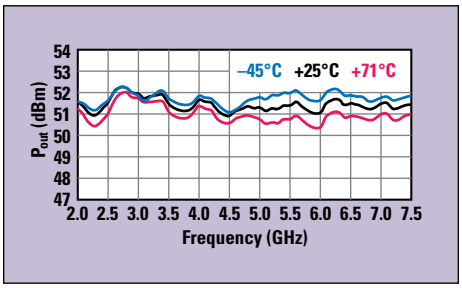

▲ **Fig. 3 Measured output power of the Spatium amplifier that combines 16 QPA1003P MMICs.**

Another operational benefit of a solid-state transmitter is the reduced harmonic content in the output signal. A solid-state PA that operates over an octave or greater bandwidth will typically have worst-case harmonic content about 8 dB down from the fundamental at its saturated output power. The harmonic content of a vacuum tube will only be down 2 dB from the fundamental under the same operating conditions. These higher harmonics can impose stricter filtering requirements for the transmitter, driving larger and costlier components for the overall ECM system.

POWERING UP WITH GaN

While GaN devices have significantly increased the power density, power and bandwidth over other heterojunction semiconductor technologies, a single device or MMIC still has insufficient power for most ECM system transmitters. It is not unusual to have a requirement of 100 W or more from 2 to 7.5 GHz. ***Figure 1*** shows the output of a single Qorvo GaN power MMIC. This packaged MMIC nominally delivers 10 W from 1 to 8 GHz, but the output power decreases at 85°C backside temperature to as low as 8 W. More than 10 of these MMICs must be combined to deliver 100 W across the band and over the temperature range required in an ECM system.

There are many ways to power combine devices to make a SSPA. For an ECM system transmitter, the approach must have low loss and wide bandwidth. Many combining techniques use two-port binary combiners such as Wilkinson or magic tees. Combining two MMICs requires a single two-port combiner, four MMICs requires three combiners and 16-way combining requires 15 combining elements. Magic tees have relatively low loss; however, they typically operate over a maximum of 10 percent bandwidth, and double-ridged magic tees only have about an octave bandwidth, which is short of a 2 to 7.5 GHz ECM requirement. With two-way combining, four stages of combining are needed to achieve the desired power. A typical double-ridge magic tee has 0.3 dB of loss at these frequencies, so the total loss through the combiner would be 1.2 dB. Combining the 30 percent efficient GaN PA MMICs shown in Figure 1 through a 16-way magic tee, the efficiency of the combined output would be about 23 percent and deliver approximately 95 W output at 6 GHz at 85°C. However, the typical double-ridge magic tee network only works over an octave of bandwidth (e.g., from 2 to 4 GHz).

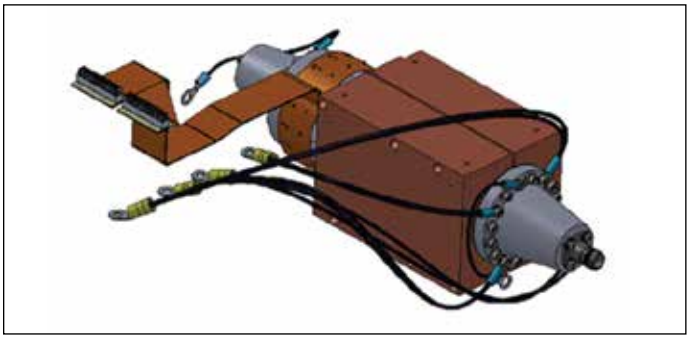

▲ **Fig. 4 Spatium amplifier with clamp to conduct heat from the MMIC PAs.**

SPATIAL COMBINING

Spatial combining techniques are potentially lower loss than circuit-based techniques. Spatium® is Qorvo's patented coaxial spatial method of power combining (see ***Figure 2***). It uses broadband antipodal finline antennas as the launch to and from the coaxial mode, splitting into multiple microstrip circuits, then combining the power from those circuits after amplification with a power MMIC. It uniquely enables broadband, efficient and compact combining of multiple power MMICs in a single combining step, with free space as the combining medium. A typical Spatium design combines 16 devices in one step, with a combining loss of only 0.5 dB.

Combining 16 of the MMICs from Figure 1 yields an SSPA efficiency of 27 percent, compared to 30 percent for each MMIC. This is a significant difference compared to the 23 percent achieved with magic tee combining. The increased combining efficiency enables higher output power from a given prime power as well as reducing the heat dissipation.

An actual Spatium amplifier was designed that combined 16 radial blades with the Qorvo GaN MMIC PA on each blade. ***Figure 3*** shows the measured output power versus clamp surface temperature; the baseplate temperature below the MMIC is approximately 12°C hotter than the clamp temperature, so the maximum baseplate temperature is 85°C. This unit achieves greater than 100 W from 2 to 7.5 GHz and an average efficiency of 25 percent.

THERMAL DESIGN

Thermal management is one of the design challenges when using a solid-state amplifier in an ECM transmitter. In a typical application, the outer surface of the clamp around the Spatium SSPA is conduction cooled on one or more sides (see ***Figure 4***). For some systems, a liquid coolant may be available, for others a heat sink with fans. The clamp

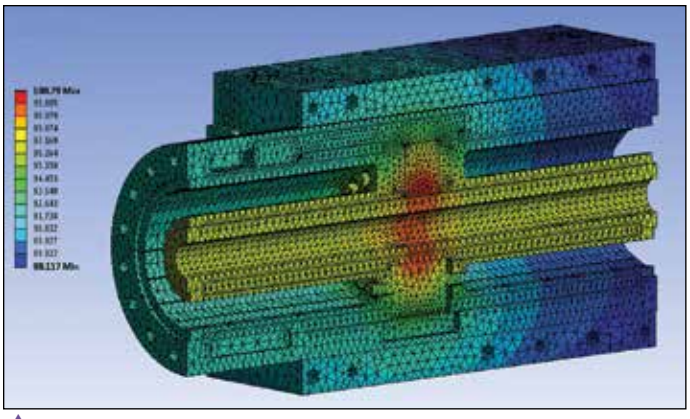

Fig. 5 Thermal simulation of the Spatium SSPA, showing cross section of the construction.

is designed to make contact with all of the blades in the Spatium and provide a conduction path to a cold plate or heat sink. Spatium blades and clamps can be made of different metals, including aluminum and copper. Size, weight and power trade-offs determine the appropriate material set for a given application.

The thermal resistance from the back of the MMICs to the mounting plates can be calculated and used to derive the backside MMIC temperature. From the thermal resistance of the MMIC and package, the junction temperature of the MMIC can be calculated and, from that, the reliability of the SSPA can be estimated. ***Figure 5*** is a thermal simulation of the SSPA shown in Figure 4, with the MMICs operating at saturated output power and the worst-case efficiency within the frequency band (i.e., 25 W dissipated per MMIC). The thermal model shows an approximate 12°C rise from the coolest spot of the outside surface of the clamp to the backside of the packaged MMIC and an additional 164°C temperature rise from the back of the package to the junction of the output transistor, assuming 6.56°C/W thermal resistance. The junction temperature of the MMIC is estimated to be 247°C with the surface of the clamp held to 71°C. At 247°C junction temperature, the MTBF of the MMIC is some 1.2 million hours.

The MTBF of the overall Spatium module will be the MTBF of the individual MMICs divided by the number of MMICs: 75,000 hours. The calculation deems a single MMIC failure to be a failure of the entire amplifier assembly—a worst-case assumption since the Spatium amplifier will gracefully degrade with the failure of any individual MMIC (i.e., approximately 0.7 dB reduction in output power per MMIC failure).

For a TWT, MIL-HDBK-217F Notice 2 provides the following formula to calculate the MTBF in a ground fixed environment:

$$\text{MTBF} = \frac{10^6}{16.5 \times (1.00001)^P \times (1.1)^F} \quad (1)$$

where P is the rated power in watts, from 1 mW to 40 kW, and F is the operating frequency in GHz, from 100 MHz to 18 GHz. Utilizing this formula, a TWT with an output power of 150 W at a frequency of 7.5 GHz has an MTBF of 29,609 hours. This is 2.5x lower than that of the comparable solid-state Spatium power amplifier module under similar environmental conditions.

SUMMARY

For the first time, GaN MMICs and broadband spatial combining techniques such as Spatium allow ECM system designers to use reliable, solid-state amplifiers instead of TWTAs. The ability to deliver hundreds of watts over broad bandwidths, while staying within the prime power available from the platform and dissipating the heat to ensure reliable operation, opens up new system opportunities for a solid-state ECM transmitter. ***Table 1*** shows the frequency, power and efficiency achieved with three recent Spatium amplifiers. The size and weight of these SSPAs are less than the boxes previously occupied by their respective TWTAs.■

TABLE 1

DEMONSTRATED SPATIUM SSPA PERFORMANCE

Frequency Range (GHz)	*Nominal Output Power (W)*	*Nominal Power-Added Efficiency*
2 to 6	300	30%
2 to 8	150	25%
2 to 18	60	15%

Yes we GaN

Boonton RF/microwave benchtop power meters and USB power sensors are ideal for testing GaN amplifier performance with best-in-class rise time, acquisition speed, time resolution, and usability to enable a wide variety of measurements, including:

- Gain
- $P_{1\ dB}$ compression
- Linearity
- Dynamic range
- Reflected power
- Stability over time

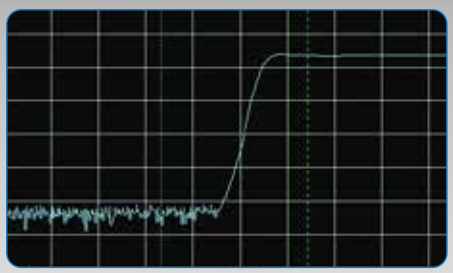

Utilize the industry-best rise time (<3 ns) and time resolution (100 ps) to characterize even the most demanding radar and communication signals.

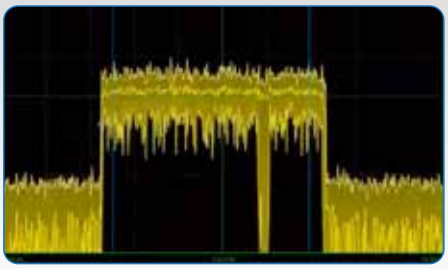

Unique *Real-Time Power Processing™* enables up to 100,000 measurements per second with virtually no missed pulses or signal anomalies.

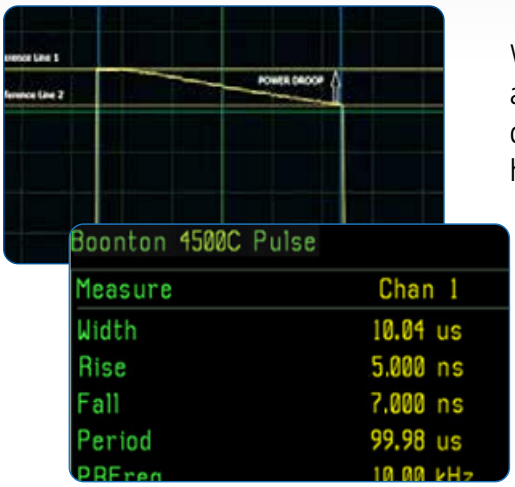

With 16 automated pulse measurements as well as various marker measurements, including droop, characterizing the performance of GaN amplifiers has never been easier.

Leaders in Power Measurement for more than 70 Years

Boonton

www.boonton.com

GaN Powers Microwave Point-to-Point Radios

Kristoffer Andersson, David Gustafsson and Jonas Hansryd
Ericsson, Gothenburg, Sweden

Gallium arsenide (GaAs) has been the key technology enabler for high performance power amplifiers and receiver low noise amplifiers in the microwave frequency bands; however, the maturity of gallium nitride (GaN) technology provides an opportunity for substantial system level improvements. The high dielectric breakdown field of GaN results in higher voltage operation and hence higher power densities. With the help of GaN, the efficiency and the maximum output power of a microwave radio can be substantially increased — directly impacting the network cost of ownership. Today, GaN monolithic microwave integrated circuits (MMIC) are being introduced in commercial microwave radios.

Today there are as many mobile subscriptions as there are people in the world and the number of subscribers, which now includes machines and things, is rising at an increasing rate. High performance microwave radios have been key enablers in achieving the successful rollout of mobile networks. By 2020 it is expected that 65 percent of the radio base station sites (excluding China, Japan, Taiwan and South Korea) will be connected to a core network via a microwave radio.[1]

The major advantages of microwave radios are fast time-to-market and low cost of ownership. Two important parameters influencing cost of ownership are energy efficiency and system gain. Increasing the system gain allows for the use of smaller antennas while maintaining capacity and link availability. Cost of ownership is typically dominated by site rental which often represents 30 to 50 percent of the total cost.[2] A small antenna size results in a lower rental cost due to reduced wind loading of the mast. This also leaves room for additional radio links.

There are a number of components in the radio system enabling improved system performance such as high gain/high efficiency power amplifiers (PA), low noise receiver amplifiers (LNA) and error correction codes that regenerate incoming signals and mitigate disturbances such as interference, noise and spurious.

The available frequency bands for microwave radio span from 6 to 70/80 GHz with a total available bandwidth of about 40 GHz. For the traditional microwave bands (6 to 42 GHz), available channel bandwidths vary from a few MHz up to 112 MHz at the highest carrier frequencies. At 70/80 GHz, the channel bandwidth is wider than 1 GHz. To use the available spectrum in the most efficient way, modern radio systems often support modulation formats up to 4096-QAM. ***Figure 1*** shows the use of different frequency bands for microwave radio applications around the world. The most used bands are between 15 and 23 GHz.

GaN MMIC TECHNOLOGY

GaN comes with the distinct advantages of high output power density and high voltage operation. From a power amplifier perspective, GaN is a game changer. Using the same size transistors, it is possible to boost output power by at least four times compared to GaAs. Higher

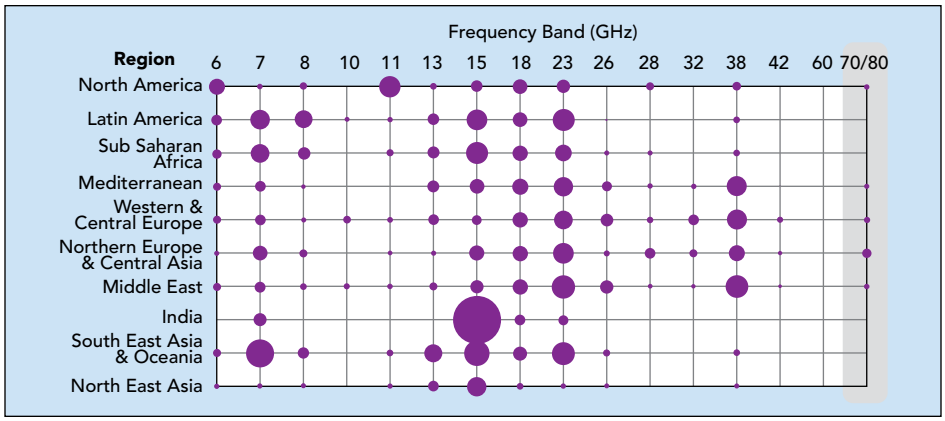

Fig. 1 Microwave radio market share vs. frequency band vs. geographic region.[3]

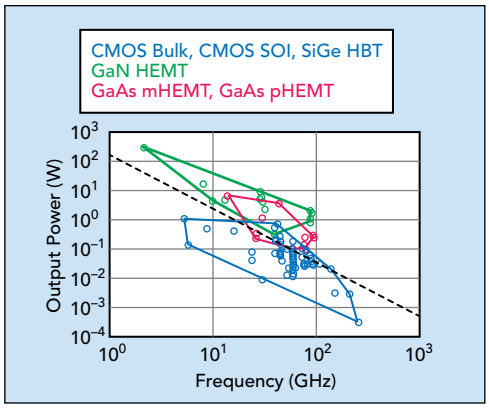

Fig. 2 Published power amplifier output power, reflecting capability of silicon, GaAs and GaN technologies.

power density means less complex circuitry, hence higher efficiency and wider bandwidth. Several semiconductor companies now have access to GaN MMIC technology offering high performance processes with gate lengths less than 150 nm. This enables high performance MMICs to greater than 40 GHz. ***Figure 2*** shows the potential of GaN power amplifiers compared to other semiconductor technologies. The figure shows regions of maximum output power versus frequency for published power amplifiers using three different semiconductor technologies (GaN, GaAs and silicon CMOS/SiGe). The dashed line shows a drop in power capability as a function of frequency for all technologies.

Existing barriers to wide-scale adoption of GaN technology in microwave point-to-point links is wafer pricing, packaging and memory effects due to trapping. The current generation of GaN MMICs is manufactured on semi-insulating silicon carbide (SiC) substrates. This technology provides the highest performance but not the most attractive price. Today the industry is moving to 6-inch SiC substrates, which helps push cost towards similar levels as GaAs. To further reduce cost, several companies are focusing on GaN-on-Silicon (GaN-on-Si) technology. GaN-on-Si is not as mature as GaN-on-SiC, however, and the performance will not be as high. One reason is the lower thermal conductivity of Si compared to SiC.

For telecommunication equipment, organic overmold packaging is the dominant technology due to its low cost and high reliability. However, only a very limited number of suppliers currently offer GaN MMICs with the necessary surface passivation to support organic overmold packaging.

Trapping in the GaN transistor may result in dynamic effects with slow time constants in the range of milliseconds to seconds.[19] The effects can appear as abrupt changes in small-signal gain following high output power events. This is more of an issue for radio base stations having very bursty traffic patterns than for microwave radio links where output power changes less rapidly.

MICROWAVE RADIO POWER AMPLIFIERS

A power amplifier is at maximum efficiency when operating at peak output power, while lowering the output power will significantly reduce efficiency. For linearity, the converse is true; the most linear operation is achieved at low output power. To mitigate the impairments associated with high efficiency operation, digital predistortion (DPD) techniques are used to compensate for power amplifier nonlinearities.

Power amplifiers for radio base stations are typically optimized for efficiency; power-added efficiencies as high as 50 to 70 percent are not uncommon. Linearity is then recovered using DPD techniques. This focus on efficiency is motivated by the high output powers (100 W average) of these base station systems. Even a moderate increase in power-added efficiency leads to a significant reduction in power consumption and cooling requirements.

Power amplifiers in microwave radios for point-to-point communications are operated Class AB to support high order modulation schemes (up to 4096-QAM). If a DPD system is available, it is typically used to enable high order modulation rather than for boosting efficiency. The maximum saturated output power for a GaAs MMIC amplifier is about 40 dBm up to 10 GHz, falling to about 26 dBm at 86 GHz (E-Band). The associated maximum efficiency is about 35 percent up to 10 GHz and about 15 percent at 86 GHz. For linear operation (i.e. 10 dB from saturation), these efficiencies drop rapidly to below 10% (3% to 10% depending on frequency). These power levels represent what is possible to achieve in a commercial setting. Striving for higher output power increases cost and power consumption.

For most point-to-point frequency bands, there are a number of organic packaged GaAs MMIC power amplifiers. For the lower frequencies, saturated output power typically lies in the range of 2 to 4 W and the power-added

TABLE 1

TYPICAL PERFORMANCE OF PACKAGED GaAs CLASS AB POWER AMPLIFIERS

Reference	Frequency (GHz)	Saturated Output Power (dBm)	P_{1dB} (dBm)	Third Order Intercept Point (dBm)	Power-Added Efficiency for Linear Operation (%)	Supply Voltage (V)
4	7	35	34	43	< 5	6
5	23	33	31	38	< 3	6
6	38	28	27	38	< 2	4

TABLE 2

PERFORMANCE OF GaN DOHERTY POWER AMPLIFIERS ABOVE 6 GHz

Reference	Frequency (GHz)	Saturated Output Power (dBm)	Power-Added Efficiency for Linear Operation (%)	Supply Voltage (V)	Physical Configuration
9	7	36	31 - 39	28	Bare Die
11	7	35	35	20	Bare Die
14	7	38	36	28	Bare Die
17	7	42	21	28	Packaged
15	10	36	34	20	Bare Die
16	23	37	27	20	Bare Die

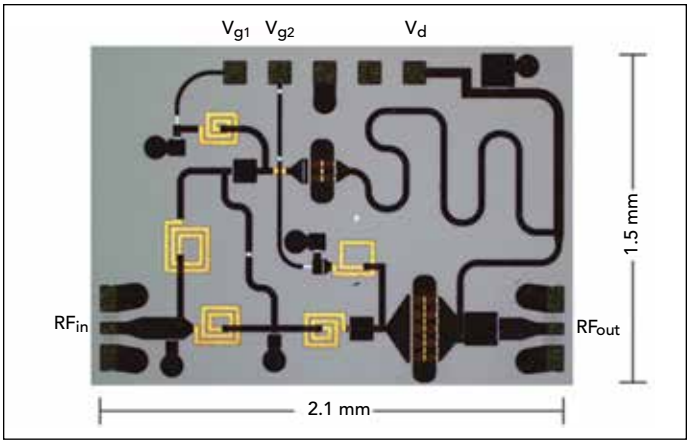

▲ **Fig. 3 7 GHz GaN MMIC Doherty amplifier.[11]**

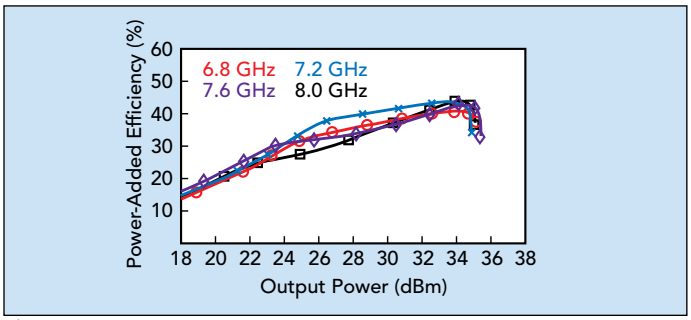

▲ **Fig. 4 Power-added efficiency of 7 GHz GaN MMIC Doherty amplifier.[11]**

efficiency for linear operation is slightly less than 5 percent. ***Table 1*** shows the typical performance of commercially available packaged GaAs Class AB power amplifiers. Taken from vendor datasheets, it serves as an illustration of the current state for point-to-point amplifiers: linear operation at the expense of efficiency.

Efficient Point-to-Point Communications Power Amplifiers

Wireless radio base stations have for some time been equipped with Doherty power amplifiers that provide high efficiency in both saturation and in back-off.[7,8] In its most basic form, the Doherty amplifier improves efficiency in back-off by using two parallel amplifier branches: a carrier amplifier and a peaking amplifier. The carrier amplifier is connected to the peaking amplifier via an impedance inverter and the peaking amplifier is then connected to the load. This arrangement at low power presents a high impedance to the carrier amplifier, which decreases as the power increases. This load modulation ensures that the carrier amplifier operates near saturation (and hence at high efficiency) over a wide range of output powers—typically 6 dB or more. Although the theoretical Doherty amplifier is a linear amplifier, the practical realization is inevitably very nonlinear. Hence, the radio base station is also equipped with a digital predistortion system that provides linear operation.

Given the success of the Doherty amplifier in the radio base station market, there have been attempts to carry over the Doherty technology to the point-to-point segment. The principal circuit level challenges have been the shorter wavelengths in the point-to-point communication bands and the low power density of GaAs. Shorter wavelengths necessitate an integrated solution in contrast to the sub-6 GHz Doherty amplifiers, where the combiner and splitting networks are implemented on the amplifier printed circuit board. The low power density of GaAs puts a limit on the maximum output that can be achieved. With the advent of short gate length GaN MMIC technology, it is finally possible to realize Doherty power amplifiers beyond 6 GHz, delivering more than 10 W in saturation.

Recent work with GaN Doherty power amplifiers operating primarily in the 7 GHz bands[9-15] and at 23 GHz[16] show that state-of-the-art GaN technology is capable of achieving a power-added efficiency of 30 percent (with 8 to 9 dB back-off) and more than 20 W of saturated output power (see ***Table 2***). In 2012, Gustafsson et al.,[11] demonstrated the performance of a GaN MMIC Doherty power amplifier operating in a microwave radio band (see ***Figure 3***). ***Figure 4*** shows its efficiency. Using a DPD system, the amplifier achieved an average efficiency of greater than 35 percent while keeping its adjacent channel leakage power ratio (ACLR) below -48 dB for a 10 MHz 256-QAM signal.

More recently, Gustafsson et al.,[17] demonstrated the performance of a GaN hybrid Doherty amplifier. The hybrid approach with passive GaAs for matching circuits limits the GaN content, which has the potential to lower the cost of the Doherty amplifier. The two-stage hybrid amplifier consists of an integrated passive GaAs input, interstage and output matching circuits and GaN power bars for the ampli-

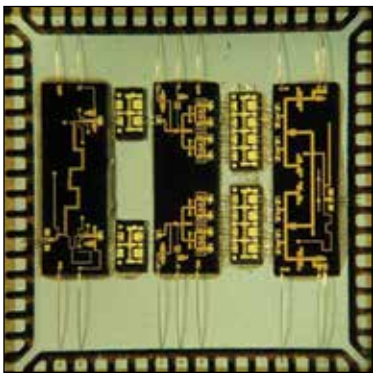

▲ **Fig. 5 GaN hybrid power amplifier before overmold application.[17] The power transistors are GaN HEMTs, and the passive input, interstage and output networks are fabricated in GaAs.**

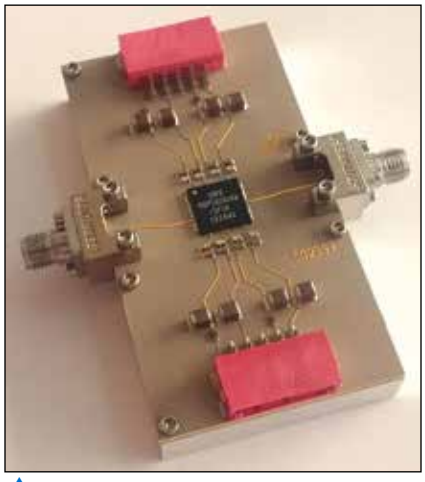

Fig. 6 Packaged GaN hybrid power amplifier mounted to an evaluation board.[17]

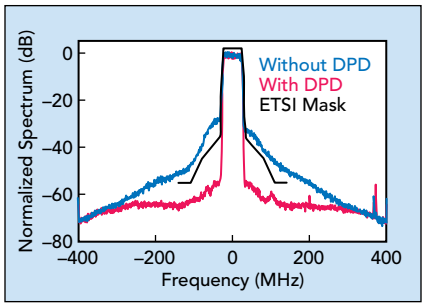

Fig. 7 Measured output spectrum of a GaN hybrid power amplifier, with and without DPD, driven by a 50 MHz, 4096-QAM input at 6.65 GHz.[17]

fier stages. ***Figures 5*** and ***6*** show the inside of the package and the packaged amplifier, respectively. Using a DPD system, the amplifier delivered 34 dBm average output power with a 50 MHz 4096-QAM signal at an average power-added efficiency of 20 percent, while fulfilling Class 8B ETSI spectral requirements[18] (see ***Figure 7***). Linearization was performed using direct learning table DPD (24 tables, 16 bins) with least square estimation of the table coefficients.

This demonstration shows that GaN and Doherty operation can increase the efficiency well beyond what is achievable in GaAs. As previously mentioned, the Doherty amplifier must be augmented with DPD. The wide bandwidth of point-to-point channels—up to 112 MHz for the traditional microwave bands —puts tough requirements on the digital predistortion system. To compensate for seventh-order nonlinearities, digital-to-analog converters should run with at least 7x oversampling (i.e., > 784 MHz). The same goes for the analog-to-digital converter in the local observation receiver (>784 MSPS). In addition to high data rates, vertical resolution should be high enough to support very high modulation rates (i.e., 4096-QAM). These data converters have been historically power hungry and, thus, the efficiency of the whole radio system is compromised. By using state-of-the-art data converters, however, it is now feasible to design digital predistortion systems with low enough power consumption.

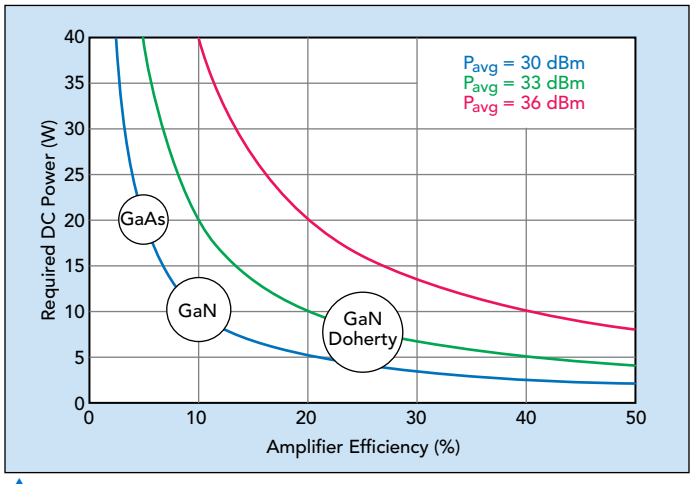

Fig. 8 DC power consumption vs. amplifier efficiency and average output power. Circled regions show typical performance of GaAs Class AB, GaN Class AB and GaN Doherty power amplifiers.

The Promise of GaN PAs in Microwave Point-to-Point Radios

There are two main uses for GaN in commercial microwave radios. The first is to leverage power density to increase output power and, thus, system gain. Using short gate length GaN MMIC processes (e.g., 0.15 μm), it is possible to substantially increase output power, compared to GaAs, up to at least 23 GHz. This comes at the cost of increased power consumption, as amplifier efficiencies are expected to improve marginally. The other use is to improve efficiency by introducing high efficiency power amplifier architectures (e.g., Doherty). With a high efficiency amplifier, it is possible to increase output power while also decreasing power consumption. Furthermore, the thermal footprint of the amplifier is reduced, enabling simpler cooling solutions.

Figure 8 shows the required DC power as a function of power amplifier efficiency for three different average power levels (30, 33 and 36 dBm). The circled areas indicate typical performance regions for GaAs Class AB, GaN Class AB and GaN Doherty power amplifiers. By replacing GaAs with GaN, an incremental increase in efficiency is achieved. At these relatively low efficiencies, however, even an incremental increase leads to substantial power savings. An increase from 5 to 10 percent power-added efficiency can reduce power consumption by 10 W and, hence, lower the total cost of ownership. The use of GaN Doherty power amplifiers enables power-added efficiencies in the range of 25 percent. This not only decreases power consumption but also increases system gain and output power.

Looking at GaN opportunities in terms of carrier frequency, there are two distinct regions (see ***Figure 9***). The first is at lower frequencies (up to about 13 GHz), where efficient Doherty operation has been demonstrated. Here one can take advantage of increased efficiency and reduced energy consumption or increased output power without increased power consumption or an enlarged thermal footprint. This region utilizes the full potential of GaN technology. The gray area indicates a transition region

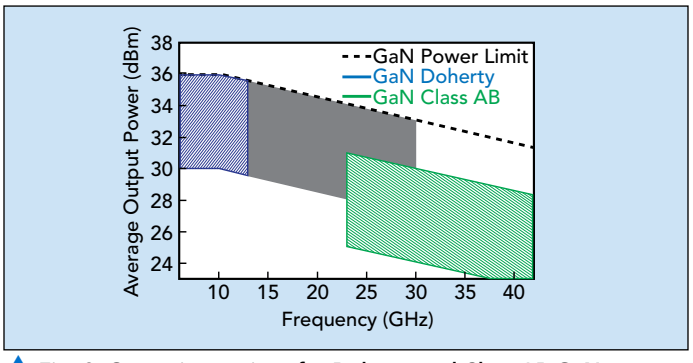

Fig. 9 Operating regions for Doherty and Class AB GaN power amplifiers.

between Doherty and Class AB power amplifiers; which technology is best to use depends on the efficiencies that can be achieved from Doherty amplifiers above 15 GHz. For the higher frequency bands (18 GHz and above), it is now possible to replace existing GaAs power amplifiers with high power GaN versions to increase output power.

CONCLUSION

GaN technology is now being introduced in commercial microwave radios. While the first wave of products provides only an incremental reduction in power consumption, Doherty amplifiers at microwave frequencies enabled by GaN and high performance data conversion technology will, in the coming years, provide power and efficiency improvements, just as they have for the base station market. ■

References

1. Ericsson, "*Microwave Towards 2020- 2015 Edition*," September 2015.
2. Ericsson, "*Microwave Towards 2020- 2014 Edition*," 2014.
3. J. Edstam, "Microwave Backhaul Gets a Boost with Multiband," *Ericsson Technology Review*, January 2016.
4. "TGA2701-SM Datasheet," www.triquint.com/products/p/TGA2701-SM.
5. "CHA5356-QGG Datasheet," http://module-csums.cognix-systems.com/telechargement/9-35-1.pdf.
6. "MAAP-011170 Datasheet," http://cdn.macom.com/datasheets/MAAP-011170_V3.pdf.
7. R. Pengelly, C. Fager and M. Ozen, "Doherty's Legacy: A History of the Doherty Power Amplifier from 1936 to the Present Day," *IEEE Microwave Magazine*, Vol. 17, No. 2, February 2016, pp. 41–58.
8. V. Camarchia, M. Pirola, R. Quaglia, S. Jee, Y. Cho and B. Kim, "The Doherty Power Amplifier: Review of Recent Solutions and Trends," *IEEE Transactions on Microwave Theory and Techniques*, Vol. 63, No. 2, February 2015, pp. 559–571.
9. D. Gustafsson, J. C. Cahuana, D. Kuylenstierna, I. Angelov and C. Fager, "A GaN MMIC Modified Doherty PA with Large Bandwidth and Reconfigurable Efficiency," *IEEE Transactions on Microwave Theory and Techniques*, Vol. 62, No. 12, December 2014, pp. 3006–3016.
10. D. Gustafsson, C. M. Andersson and C. Fager, "A Modified Doherty Power Amplifier with Extended Bandwidth and Reconfigurable Efficiency," *IEEE Transactions on Microwave Theory and Techniques*, Vol. 61, No. 1, January 2013, pp. 533–542.
11. D. Gustafsson, J. C. Cahuana, D. Kuylenstierna, I. Angelov, N. Rorsman and C. Fager, "A Wideband and Compact GaN MMIC Doherty Amplifier for Microwave Link Applications," *IEEE Transactions on Microwave Theory and Techniques*, Vol. 61, No. 2, February 2013, pp. 922–930.
12. R. Quaglia, V. Camarchia, M. Pirola, J. J. M. Rubio and G. Ghione, "Linear GaN MMIC Combined Power Amplifiers for 7-GHz Microwave Backhaul," *IEEE Transactions on Microwave Theory and Techniques*, Vol. 62, No. 11, November 2014, pp. 2700–2710.
13. V. Camarchia, J. Fang, J. M. Rubio, M. Pirola and R. Quaglia, "7 GHz MMIC GaN Doherty Power Amplifier with 47 Percent Efficiency at 7 dB Output Back-Off," *IEEE Microwave and Wireless Components Letters*, Vol. 23, No. 1, January 2013, pp. 34–36.
14. V. Camarchia, J. J. M. Rubio, M. Pirola, R. Quaglia, P. Colantonio, F. Giannini, R. Giofre, L. Piazzon, T. Emanuelsson and T. Wegeland, "High-Efficiency 7 GHz Doherty GaN MMIC Power Amplifiers for Microwave Backhaul Radio Links," *IEEE Transactions on Electron Devices*, Vol. 60, No. 10, October 2013, pp. 3592–3595.
15. M. Coffey, P. MomenRoodaki, A. Zai and Z. Popovic, "A 4.2-W 10-GHz GaN MMIC Doherty Power Amplifier," *IEEE Compound Semiconductor Integrated Circuit Symposium*, October 2015, pp. 1–4.
16. C. F. Campbell, K. Tran, M. Y. Kao and S. Nayak, "A K-Band 5W Doherty Amplifier MMIC Utilizing 0.15µm GaN on SiC HEMT Technology," *IEEE Compound Semiconductor Integrated Circuit Symposium*, October 2012, pp. 1–4.
17. D. Gustafsson, K. Andersson, A. Leidenhed, A. Rhodin and T. Wegeland, "A Packaged Hybrid Doherty PA for Microwave Links," *European Microwave Week*, October 2016.
18. "ETSI-EN 302 217-2-2 V2.2.1 (2014-04)," www.etsi.org/deliver/etsi_en/302200_302299/3022170202/02.02.01_60/en_3022170202v020201p.pdf.
19. Jungwoo Joh and Jesús A. Del Alamo, "A Current-Transient Methodology for Trap Analysis for GaN High Electron Mobility Transistors," *IEEE Transactions on Electron Devices* 58.1, 2011, pp. 132-140.

Mastering the Thermal Challenges of Advanced Defense Subsystems

Duncan Bosworth and Gary Wenger
Analog Devices Inc., Norwood, Mass.

With the continued drive to smaller form factor, such as smaller munitions and unmanned systems, the defense world is pushing the boundaries of electronic system integration and processing densities. Although smaller and smaller footprints are now becoming a reality, the challenge of thermal dissipation is often not considered. Yet meeting the thermal challenges, to ensure long term reliability and repeatable system performance, is becoming a more significant part of the system design, particularly considering the extreme temperature ranges over which many aerospace and defense systems must operate. To meet system size, weight and power (SWaP) needs, an increasing proportion of system design time needs to be allocated to the thermal challenges.

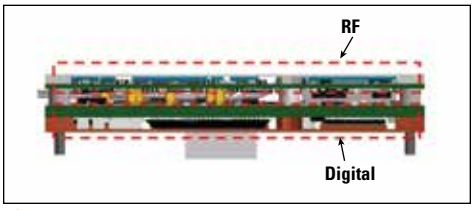

Fig. 1 A receiver module with integrated RF and digital subsystems. The module is 3.25" × 0.5" × 1.4" and dissipates 27 W in the RF section and 22 W in the digital section.

Consider a typical RF receiver and transmitter ***(see Figure 1),*** which could be the basis for a military radio, element digitization for a radar system or a communications link for an UAV or advanced munition. Depending on the frequency of operation and specific application, the system requires the integration of a number of functions and technologies to achieve optimum performance. The RF front-end requires power and low noise amplifiers, most likely based on GaAs or GaN. The mixing stages, intermediate amplifiers and synthesizers will be developed using GaAs or SiGe, with the digitizers and FPGA nodes on CMOS. This may result in four or five different technologies across the signal chain, with many more variations of process geometries. Integrating these can result in the need to dissipate 50 W or more in a few square inches and limited thermal pathways. GaN-based power amplifiers (PA), widely used in radar and electronic warfare (EW) systems, present other challenges with their system requirements and power density. For example, the PA shown in ***Figure 2*** integrates two GaN MMICs, each dissipating 80 W. Multiple PAs are grouped close together to increase overall power.

To optimize SWaP and cost, a thorough understanding of the thermal design is necessary to keep the temperatures of critical components within their operating bounds. Each technology and application has its own challenges from a thermal perspective, and the drive to reduced

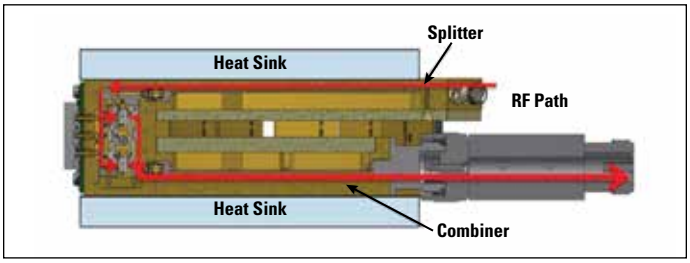

Fig. 2 Cross-section of a power amplifier combining dual, 80 W GaN MMICs.

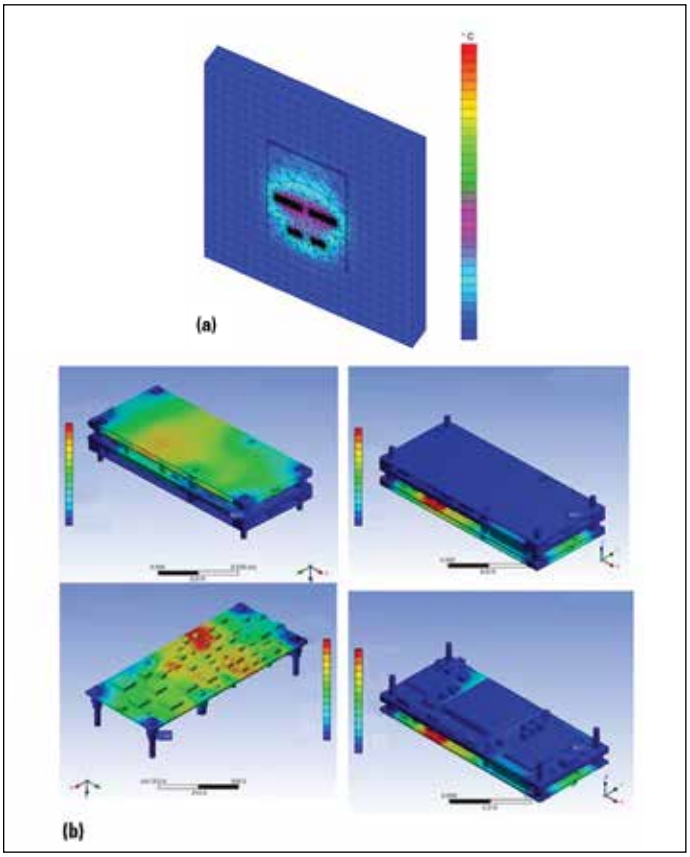

Fig. 3 Die (a) and board (b) thermal simulations.

SWaP concentrates heat densities. The dissipation needs to be reviewed from multiple perspectives, as heat generated in the channel of a MMIC flows in a continuous chain through numerous layers and interfaces until it ultimately reaches the ambient environment. The entire chain must be reviewed to optimize system thermal performance, SWaP and cost.

Although the focus on system size reduction is certainly making the thermal challenge more complex, some relief is available from advanced process nodes and increasing device integration. Advanced SiGe and CMOS nodes are enabling significant power reduction, and increasing integrated digital signal processing is increasing integration. This supports increased functionality, often at power parity with previous generation architectures. The higher operating junction temperature of GaN reduces the cooling requirements for these individual components. However, process node migration is not enough to meet the thermal challenges. System miniaturization is seemingly moving faster.

SIMULATION IS KEY

While building and testing prototypes continues to be critical in confirming design assumptions, the development times and high costs preclude efficient optimization based on hardware testing. Detailed simulation is essential and enables the rapid evaluation of multiple system variations. Trade-offs need to be evaluated from the entire system perspective. Multiple model levels and tools are required, as the geometry can scale six orders of magnitude, from sub-micron gates to meter-long housings. Heat generating and transfer mechanisms can include conduction, convection, radiation and EM energy. Simulation enables fast performance and cost trade-offs, optimizing from the device gate to system-level component placement, part design and material selection, as well as fan and heat sink specification (see ***Figure 3***).

The maximum freedom comes from system designers who have control over the entire system chain, from the MMIC gate to the ambient environment. This allows a comprehensive approach to the thermal challenges, enabling trade-offs that may change device location and require device modifications. Accomplishing this often requires multiple models and software packages. Specialized analysis techniques such as computational fluid dynamics (CFD) for convection to fluids/air and electromagnetic simulations for RF losses can be used, with a handoff between each. For example, a rack mounted, air cooled, high power, solid-state amplifier used in radar or EW systems may need the following:

- Finite element analysis (FEA) with micron-scale meshing, including die level and heat spreader analysis
- Electromagnetic loss analysis to determine the power generated in RF lines
- FEA at the chassis level
- CFD analysis for airflow and convection to the ambient environment.

The greatest temperature deltas will typically occur at the locations of greatest heat concentration, which are ultimately near the gates. Typically, 70 percent of the temperature rise from ambient to junction is within the MMIC. With GaN power densities in radar systems now above 6 W/mm in some cases, simulating the trade-offs is critical.

SELECTING THE RIGHT MATERIALS

The choice and use of very high thermal conductivity materials to spread the heat are obviously critical. For example, with high power GaN die that are used in the latest PAs for radar, the substrate is typically SiC, and the first attach layer is AuSn solder. Over just 5 mils of material, the heat flux density may reduce from 13,000 W/mm^2 to 24 W/mm^2. As the heat continues to flow through the system, spreading will continue to reduce the flux density. The choice of materials is limited by matching the coefficient of thermal expansion (CTE), electrical conductivity to ground and the cost and ability to manipulate the material.

CTE mismatches can result in cracking of substrates or delamination of bonding layers, such as solder and epoxy. Cold storage and operating temperatures, critical aspects of aerospace and defense performance criteria, tend to cause the greatest CTE stresses, as the solders and epoxy are designed for processing at elevated temperature. Even mild delamination can have catastrophic effects on the

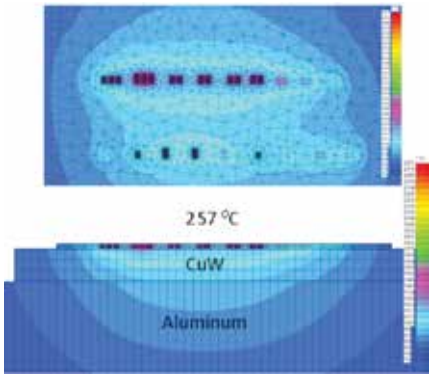

(a)

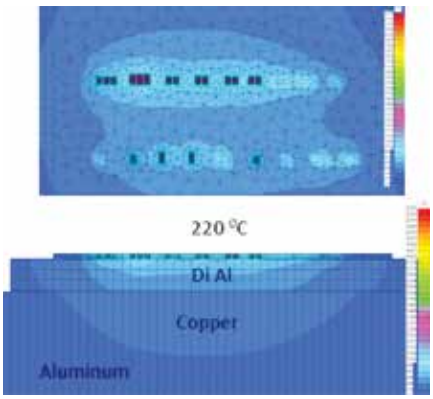

(b)

Fig. 4 Thermal performance of 60 W GaN die attached to CuW and Al (a) vs. diamond-aluminum matrix on Cu and Al (b).

thermal performance of a die, if the separation is in an area of high heat concentration — directly under a high power FET, for example. Comparing the hot spot temperatures on IR images of a design to known good images of the same design is a useful method for identifying early delamination when evaluating new materials.

Epoxy and sintered silver manufacturers are developing products with lower modulus of elasticity to absorb the CTE stresses while still retaining relatively good thermal performance. Heat conductivity close to the die is a key material research area, with extremely high thermal conductivity materials such as diamond being reviewed. As defense systems continue to look for reduced SWaP and cost, performance trade-off decisions for cost, weight and size are always intertwined in system architecture and thermal trade-offs. The use of materials such as diamond composites may seem hard to justify; however, using even small pieces of these materials as die heat spreaders in areas of high heat concentration can substantially reduce device temperatures and enable cost and weight savings in other parts of the system. ***Figure 4*** compares two thermal simulations: a 60 W GaN die attached to a CuW carrier on an aluminum base vs. a diamond-aluminum matrix material carrier on a copper insert in an aluminum base. The latter reduced the junction temperature by some 37°C, providing improved system performance and life, while enabling other SWaP and cost tradeoffs elsewhere in the system.

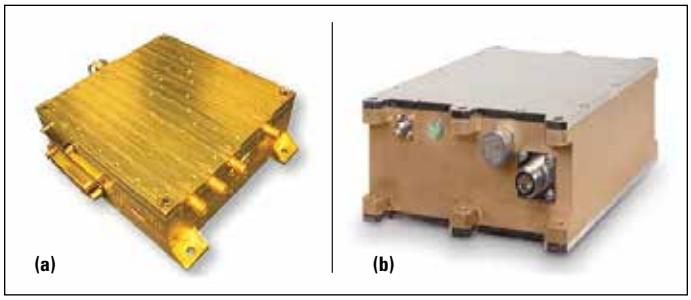

(a) (b)

Fig. 5 Examples of products using the integrated thermal design methodology: "man portable," 5 W linear PA and up-converter (a) and 2 kW HPA (b).

In other examples, convection cooled systems, such as rack mounted, can be challenged with large temperature differences across the heat sink base and from the heat sink fins to the ambient air. Heat sink and fan choices have significant cost and performance impact and must be specified from a system perspective. For a given heat sink volume, better performance is driven by a higher convective heat transfer rate that requires greater back pressure, such as from tighter channels or staggered/slotted fins that break up boundary layers. This, in turn, requires larger and more power-hungry fans. The fan choice also impacts performance. Axial fans are typically the easiest to design with, providing high volume for low pressure systems, while centrifugal fans or blowers are able to push against higher pressure but with lower volume.

Lastly, the choice of heat sink material can significantly impact cost. In many cases, skived copper heat sinks seem to provide a good balance between performance and cost. Embedded heat pipes are also excellent low weight devices for enhancing the effective thermal conductivity of heat sink baseplates, although they do not work in all environments. High g-force environments pose a particular issue.

PUTTING IT ALL TOGETHER

Although it may seem that the thermal challenges are ominous, with many trade-offs, using a systematic approach can achieve solutions that balance cost, size and performance. Advanced simulations provide the backbone for quick decisions, enabling detailed analysis from the gate in the die to the system, as well as the impact of the heat sinks and heat spreaders. These advanced simulations help with trade-offs, from materials choices to cooling techniques and optimal layout. Applying these techniques with appropriate design decisions can yield systems with high heat concentration. ***Figure 5*** shows two examples: a 37 W linear PA with integrated up-converter and a 2 kW solid-state high power amplifier (HPA). Both product designs utilized detailed simulation, which led to careful component integration, layout and material selection to balance performance and cost. The up-converter was designed to be "man portable," so minimizing size and weight was an important requirement. Having the system and MMIC designed by the same team helped in balancing reliability, cost and performance. ■

Your partners in performance

for mission critical RF systems

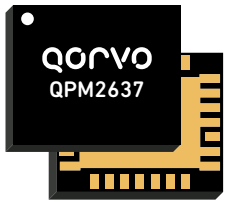

9-10.5 GHz GaN FEM for X-Band Radar Applications

This GaN FEM provides 4 functions in a single compact package: T/R switch, PA, LNA and limiter. The Rx path offers 21 dB gain with low noise figure of 2.7 dB. The Tx path offers a small signal gain of 23 dB, it can deliver 4 W of saturated power with a PAE of 38%. Designed for high temperature environments, the QPM2637 supports next-generation AESA radar. **Learn More.**

qorvo®

www.qorvo.com

For samples and orders, contact our worldwide distributor.

RFMW™

www.rfmw.com

Qorvo's GaN-on-SiC RF solutions set the standard for MTTF reliability – over 10 million hours at 200° based on more than 16,000 devices with 65 million device hours. Qorvo's GaN enables mission critical aerospace, defense and radar systems requiring smaller, more efficient solutions with longer operating life.

To learn how Qorvo GaN powers the systems all around you, visit www.qorvo.com/gan

Going Green: High Efficiency GaN Amplifiers

Patrick Hindle, Microwave Journal Editor
Microwave Journal Editor

Improving amplifier efficiency is a key goal in many systems as PAs typically consume the largest amount of energy of any component. GaN has several advantages over other technologies such as high power density, high power, high gain and high efficiency.

In order to achieve maximum efficiency, manufacturers are using modulation techniques like envelope tracking or outphasing plus DPD to reduce distortion. Applying these techniques to GaN has taken high power amplifiers to the next level for many applications and promises to greatly reduce power consumption. We asked several leading GaN device manufacturers to provide examples of their highest efficiency GaN amplifier designs as we look to a greener future.

ANALOG DEVICES - BROADBAND AND HIGH POWER A&D GaN

Norwood, Mass.

GaN is changing the RF and microwave landscape across communications systems ranging from mobile wireless networks to aerospace and defense, with most future radar, military communications and electronic warfare systems investigating its benefits. By reducing device parasitic elements, using shorter gate lengths and using higher operating voltages, GaN transistors have reached higher output power densities, wider bandwidth and improved DC to RF efficiencies. As the size of modern systems become increasingly important, GaN, with its improved power density, is up to 6× better than GaAs and provides a reduced system footprint with higher reliability.

One example of the benefit of leveraging GaN is in modern phased array radar systems. With thousands of active elements, GaN technology is providing comprehensive solutions for transmit-receive modules, enabling increased power density and integration with the PA, LNA and T/R switch all developed in GaN. The high breakdown voltage also potentially eliminates the need for the limiter — traditionally used to protect the LNA — reducing component count and area, which is critical at higher frequencies with minimal antenna aperture spacing.

GaN's higher operating impedance also enables optimized solutions for electronic surveillance and countermeasures, with a single broadband power amplifier now able to cover multi-octave bandwidths. For example, ADI's HMC7149, based on a 0.25 micron process, is

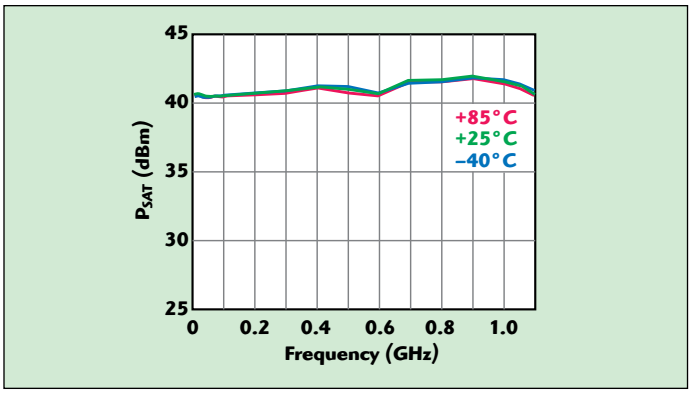

▲ **Fig. 1 HMC1099 saturated output power vs. frequency for various temperatures.**

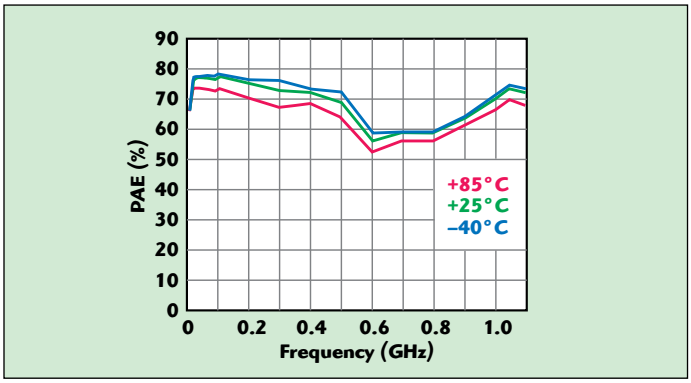

▲ **Fig. 2 HMC1099 power-added efficiency vs. frequency for various temperatures.**

able to support amplification across 6 to 18 GHz with minimal variation of output power and gain. A single PA can now be used where previous PA performance necessitated band partitioning.

Advanced power combining solutions incorporated with GaN yield even stronger benefits to users. Using proprietary power combining methods and advanced bias control/monitoring circuits in core power combined modules, ADI's SSPAs provide solutions from 100 W broadband to 8 kW at X-Band, combining up to 256 MMICs. These new system-optimized solutions for radar and electronic warfare have high efficiency and RF power density and provide alternative solutions to traditional TWTs.

Another example is a 10 W GaN amplifier which operates over an instantaneous bandwidth of 0.01 to 1.1 GHz with ± 0.5 dB of gain flatness (see ***Figure 1***). It offers high saturated output power with 69 percent typical power-added efficiency (PAE) and 18.5 dB of small signal gain (see ***Figure 2***). The device is designed for industrial and portable applications where GaN technology is needed to meet the increasing demands on battery lifetime. The device utilizes internal prematching to realize a single external matching network to provide high PAE over the full bandwidth and is packaged in a compact, low cost 5 mm × 5 mm QFN package.

After its acquisition of Hittite, ADI is taking aim at many high performance defense and aerospace applications. The company offers a broad portfolio of experience in everything from device to subsystem products and dedicated labs, production and testing facilities.

AMPLEON – HIGH EFFICIENCY CELLULAR BASE STATION GAN

Nijmegen, The Netherlands

In cellular base stations, the need to have higher throughput forces the use of higher modulation coding schemes, which leads to higher peak-to-average signals. As a consequence, the RF PA's average efficiency is reduced. One candidate architecture suitable to minimize this issue is out-phasing, where highly efficient switched-mode PAs can be used. However, its pure version has some drawbacks, namely the nulling problem and response to DPD algorithms. A solution for these issues is to split the operation into two ranges: pure out-phasing and a linear mode in the highest and lowest input power levels, respectively. The nulling problem is solved by this method, as the zero output power is achieved when the input power is also zero and not at the expense of subtracting two high power signals with opposite phase.

Ampleon has developed an out-phasing PA prototype board that uses two IAF 0.25 mm GaN transistors. A quasi load insensitive (QLI) class-E topology is chosen for its high efficiency against load modulation. The higher harmonic impedances of the transistors were matched inside the commercial RF package, SOT1135, which eases the combiner design. Since the packaged devices are not very sensitive to higher harmonic load impedances, the combiner is easier to design. A standard 30 mil Rogers substrate, RO4350B, is used for the board design.

The static CW measurements for several values of input power and phase angle using a dedicated dual input measurement system are shown in ***Figure 3***. Each line corresponds to an input power level and each dot to an out-phasing angle. It is evident that in the pure out-phasing regime, at the back-off levels, the efficiency degrades considerably. Additionally, it is interesting to see that it is possible to obtain the same output power level using different values of input power and phase angle. With this unique property, the best efficiency performance can be selected (especially in back-off) using the appropriate combination of input power and phase angle using a lookup table approach. The unique amplitude and phase points corresponding to the highest efficiency are chosen and lookup tables (phase, amplitude) are formed. This method allows not only the extension of the dynamic range (nulling issue), but also efficiency optimization.

The mixed mode, out-phasing PA was tested with a single carrier W-CDMA signal seen in ***Figures 4a*** (non-linearized) and ***4b*** (linearized). Before the linearization, the starting value of ACLR is equal to -28 dBc and the EVM 9 percent. After a single pass DPD cycle, it was possible to improve

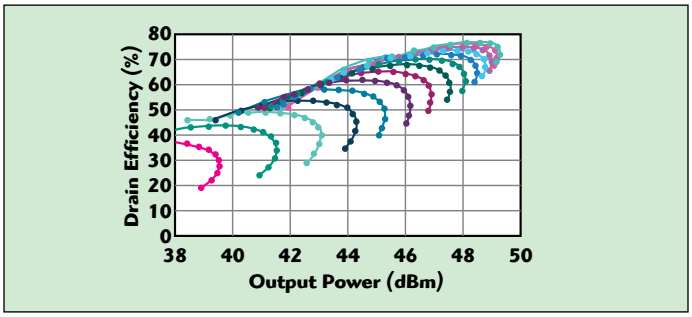

▲ **Fig. 3 Static CW measurements for various values of input power and phase angle.**

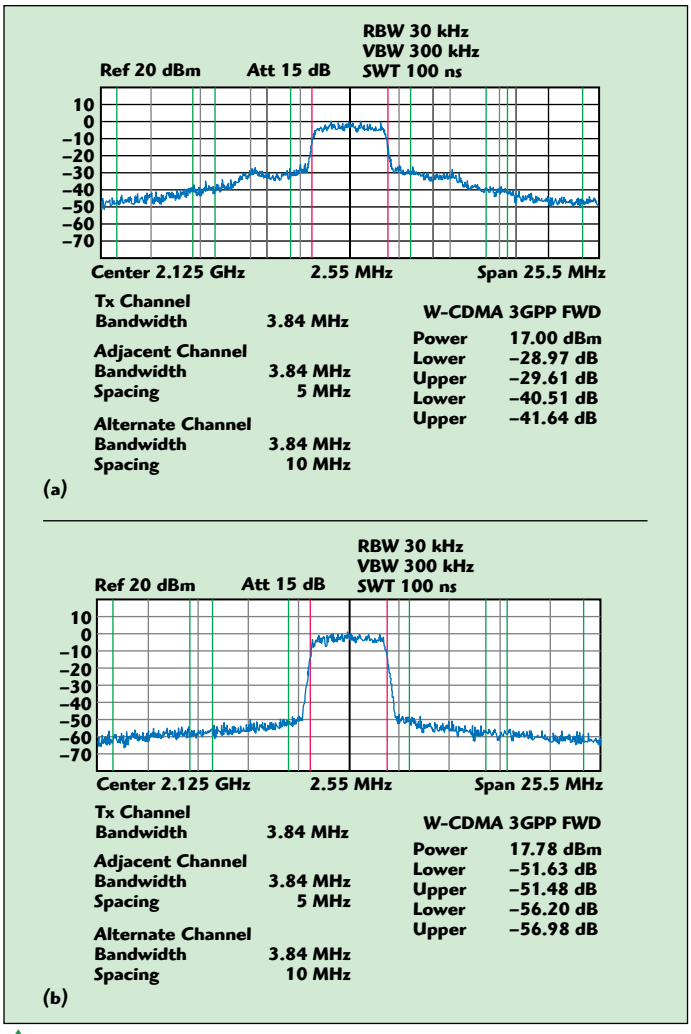

▲ **Fig. 4 W-CDMA single carrier spectrum before linearization (a) and after linearization (b).**

these values to -51 dBc and 1.1 percent, respectively. The achieved efficiency is high (>65 percent) and the PA responded to linearization algorithms, which showed the potential of the mixed mode, out-phasing concept for future high efficiency base stations.

Ampleon is the spinoff of the NXP RF power business, as NXP acquired Freescale and kept their RF power products. Ampleon is a major player in the wireless infrastructure power market, developing many unique designs to meet the next generation of RF power: the RF energy market for applications such as microwave ovens, lighting, automobile ignition systems and food processing.

MACOM – BREAKING THE MOLD WITH HIGH EFFICIENCY GaN ON Si

Lowell, Mass.

MACOM is the only RF GaN manufacturer that produces GaN on Si devices (the others use GaN on SiC). MACOM does produce devices on both substrates, putting significant focus on GaN on Si for low cost, high volume markets such as wireless infrastructure and RF energy. MACOM recently released a GaN wideband D-mode transistor optimized for 1.8 to 2.2 GHz modulated signal operation in cellular base station applications and housed in an over molded plastic package. Using MA-

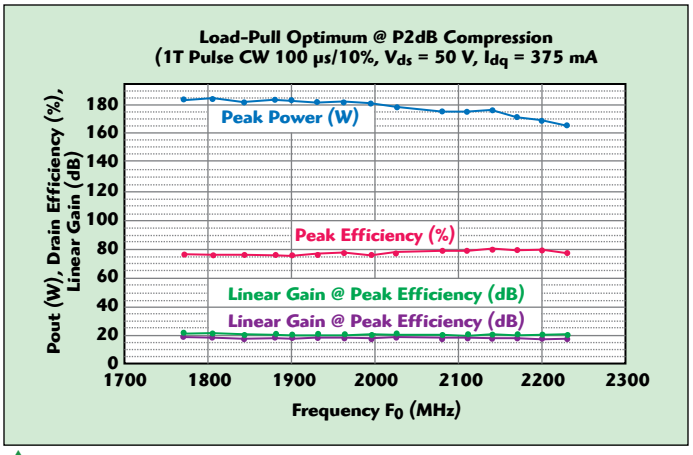

▲ **Fig. 5 Output power, gain and efficiency vs. frequency.**

COM's Gen4 GaN technology, the MAGB-101822-120B0P is one in a family of products in MACOM's MAGB series. The series enables competitive products with state-of-the-art performance for LTE base station applications at LDMOS-like cost structures (at volume). These products have been optimized to deliver high drain efficiency and linear gain and are easy to linearize using digital predistortion (DPD) according to some customers.

These products target all the cellular bands within the 1.8 to 3.8 GHz range and deliver significant power efficiency improvements, in addition to package size reduction over legacy LDMOS. The products are housed in a plastic TO-272 package, operate over 400 MHz of bandwidth, and support 30, 40 and 60 W cellular infrastructure applications. The ability of this single device to cover the cellular bands and power levels from 1.8 to 2.2 GHz would require multiple LDMOS-based products.

The device delivers 160 W of peak output power on the load-pull system (fundamental tuning only), has linear gain of 20 dB and peak efficiency of 75 percent across the full band, similar performance to the ceramic version (see ***Figure 5***). Peak efficiency can be improved to well above 80 percent when the device is presented with the proper harmonic terminations. A 2× MAGB-101822-120B0P symmetric Doherty amplifier optimized for Band 1 is capable of delivering 55 dBm of peak power. When the Doherty amplifier is measured with a two carrier 20 MHz LTE signal, a total of 40 MHz carrier, and at 7.5 dB back-off, the gain is 15.5 dB and efficiency is 55 percent. Using a commercially available DPD kit and without any special optimization, the adjacent channel power ratio (ACPR) can be easily corrected to less than -55 dBc. The Doherty amplifier achieves a video bandwidth of 200 MHz.

The device enables the implementation of a simple symmetric Doherty amplifier design without compromising RF performance, compared to less performing and complex asymmetric Doherty topologies needed when using LDMOS based transistors. The symmetric Doherty amplifier, using the MAGB-101822-120B0P, is also easy to DPD linearize, which has been a challenge for users of other GaN-based products in the market. By overcoming all the RF and thermal challenges of designing GaN-based products in a plastic molded package, this product replaces high cost ceramic air cavity packages without compromising RF and thermal performance. MACOM's improved package offer-

ing provides further system level cost savings to the customer and eliminates another barrier to full GaN adoption.

The MACOM Gen4 technology is enabling wireless carriers to deploy the latest LTE releases and significantly reduce system operating expenses at highly competitive price points, with a scalable supply chain combined with experienced applications and design support team. MACOM is qualifying this process for widescale production and also taking aim at the RF energy market.

QORVO – HIGH PERFORMANCE GaN FOR RADAR

Greensboro, N.C..

Airborne, land and naval radar platforms continue to push for higher PAE for the transmit PAs. Improving the PAE of the system can result in simplified thermal management; power supply requirement relaxation and longer Tx path pulse width operation. To meet the need for higher PAE in commercial and military radar applications at S-Band, Qorvo has developed a family of GaN PAs. All Qorvo S-Band GaN PAs have > 50 percent PAE. The latest and highest efficiency member of the S-Band family is the QPA1000, well suited to meet the needs of radar applications in the 2.8 to 3.2 GHz frequency band.

It is designed using the Qorvo QGaN25 0.25 mm GaN on SiC production process to provide >58 percent PAE and >50 W saturated power pulsed with an input power of 25 dBm (see ***Figure 6***). Measured PAE exceeds 60 percent in portions of the operating band with minimal changes to the saturated output power. The part is a two stage, near class B design with >22 dB large signal gain (see ***Figure 7***). The PA is mounted in a 7 mm × 7 mm × 0.85 mm, 48 pin molded plastic QFN surface-mount package. The PA is designed to operate at a quiescent bias point of Vd = 25 V and Idq = 200 mA. For verification testing the pulse width and duty cycle are 100 µs and 10 percent, respectively, but

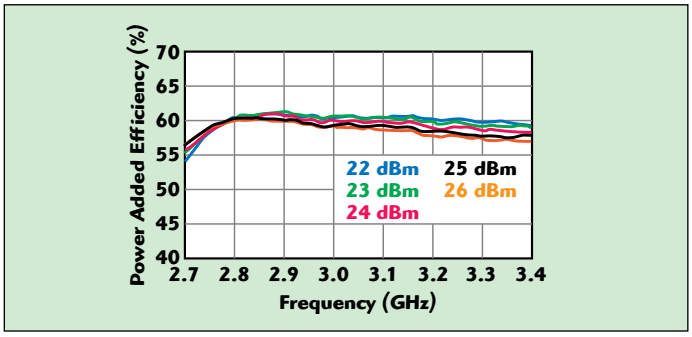

▲ Fig. 6a PAE vs. frequency: Vd = 25 V; Idq = 200 mA; PW = 100 µs, Duty Cycle = 10%.

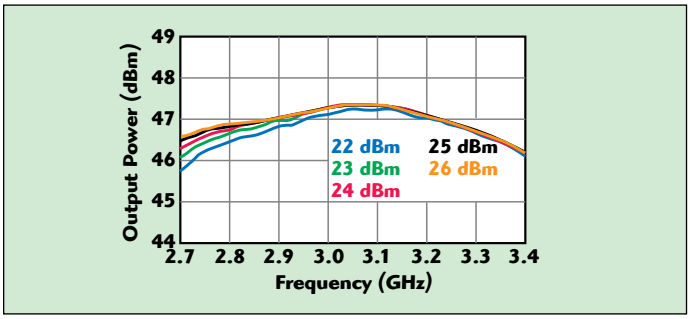

▲ Fig. 6b Output power vs. frequency: Vd = 25 V; Idq = 200 mA; PW = 100 µs, Duty Cycle = 10%.

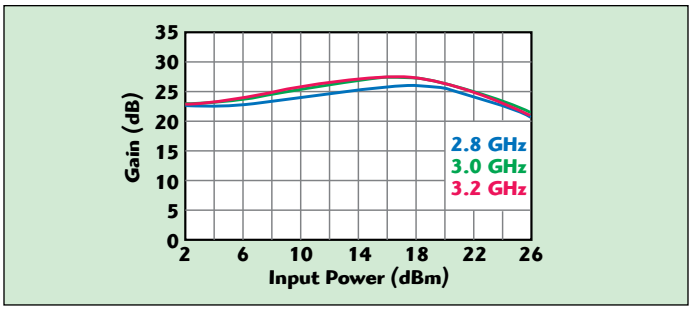

▲ Fig. 7 Large signal gain vs. input power: Vd = 25 V; Idq = 200 mA; PW = 100 µs, Duty Cycle = 10%.

it is capable of supporting a variety of operating conditions and pulse applications due to the good thermal properties.

The high PAE is achieved by optimizing the load-side impedance termination for both gain stages, and the transistor layout for both electrical and thermal performance, as well as compensating for the package parasitics. Measured load-pull data, package interface models, nonlinear transistor models, electromagnetic simulation and thermal modeling are all used to optimize the circuit. Package parasitics are determined through similar design testing, modeling and calculation.

Qorvo continues to push amplifier PAE as a critical parameter for radar applications. Operating class choice, form factor, load-pull data, model accuracy and thermal considerations all play an important role in achieving optimal overall amplifier performance.

GH EFFICIENCY GaN FOR SPACE APPLICATIONS

Osaka, Japan

Sumitomo Electric has recently qualified the SGN-15H150IV GaN device at high reliability levels for space applications. This third generation GaN device is allowing an advantage over previous technologies in gain and power levels with excellent reliability. It has 150 W (51.5 dBm) typical output power and 117 W (50.7 dBm) minimum power output at 4 dB gain compression when operated at a drain voltage of 50 V. That is the highest power level of space qualified GaN device available at this frequency, covering 1.55 to 1.6 GHz according to the company. High impedance levels allow for simple external matching circuits to meet all performance goals. A high linear gain of 17.5 dB

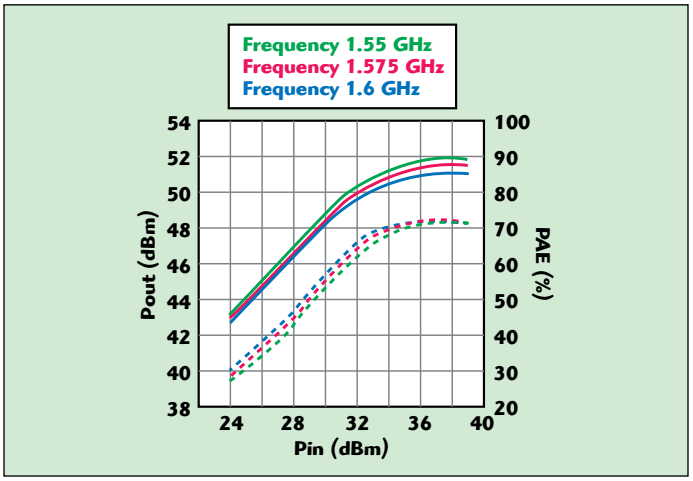

▲ Fig. 8 Ouput power and PAE vs. input power: Vd = 50 V; Idq = 500 mA; frequency 1.55 to 1.6 GHz.

minimum, 18.8 dB typical, makes driving the device easier. It has excellent PAE of 67 percent minimum (71 percent typical has been measured in an application engineering breadboard). ***Figure 8*** shows output power and PAE vs. input power.

The device has excellent performance over temperature with the classic HEMT two-slope gain shape. The inflection point is below -20°C, making gain constant from -40° to -10°C, and a slope of -0.012 dB/°C above that point. The same phenomenon makes the power constant from -40° to 25°C. The power has the same slope as the gain of -0.012 dB/°C from 25° to 85°C. PAE is approximately linear, with a slope of -0.068 percent per °C.

At 150 W output power, thermal considerations are very important. The thermal characteristics have been optimized in the device and housing structure, resulting in very low thermal resistance of 0.6 °C/W typical and 0.7 °C/W maximum. Each device is measured for thermal resistance individually and that data is delivered with the device. The maximum junction temperature is 250°C. This high maximum junction temperature allows for a conservative de-rating to 160°C operating junction temperature for safe and reliable operation.

The package is the same as the previous generation of GaAs high reliability designs, and the pre-match offers similar impedance levels as previous lower power devices. This eases upgrading current designs to take advantage of the higher output power.

For those who are attempting even higher PAE, low Cds and excellent performance at lower voltages make this device is a good candidate for envelope tracking schemes. Low on resistance along with high reverse breakdown voltage (BVgd) also makes it attractive for switch-mode designs. Nonlinear models are available as well, for more precise first-pass design and evaluation of nonlinear behavior before building the device into a design.

Primary applications would be in navigation satellites, GPS L1 Band or Galileo E1 Band. Sumitomo continues to focus on high performance satellite, radar and space applications for its GaN products.

WOLFSPEED, A CREE COMPANY
ENERGY EFFICIENT GaN FOR BASE STATIONS
Durham, N.C.

Wolfspeed is enabling designers to invent wireless systems for a responsible, energy-efficient future. Eta Devices, an MIT spin-out based in Cambridge, Mass., is pioneering the use of supply modulation through its technology called ET*Advanced*. ET*Advanced* enables base station transmitters to achieve the highest efficiency at peak power and the highest efficiency at back-off of any known technique according to the companies. And, unlike previous technologies using supply modulation, ET*Advanced* has proven to retain its advantages for both high bandwidth (multi-carrier LTE) and high linearity (MC-GSM) applications. When combined with Wolfspeed's GaN devices, the result has been reported to be the highest efficiency base station amplifiers.

ET*Advanced* solves the key power challenge facing the wireless industry today. As shown in ***Figure 9***, ET*Advanced* uses discrete supply levels to modulate the drain of a PA, making millions of transitions per second in order to optimize power consumption. At almost every place in the wireless ecosystem, the power consumption and the heat dissipation of the PA are limiting factors that increase cost and size, limit output power and range, and overtax energy supply resources.

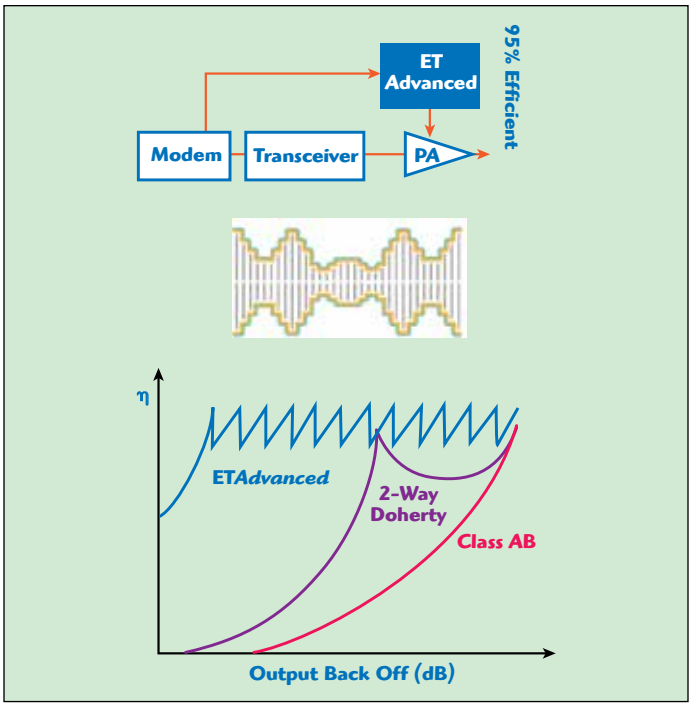

▲ **Fig. 9 ETAdvanced uses discrete supply levels to modulate the drain of a PA, making millions of transitions per second to optimize power consumption.**

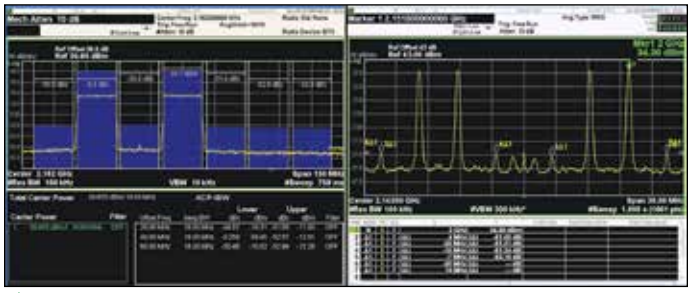

▲ **Fig. 10 Eta Devices' demonstration of LTE and MC-GSM performance using ETAdvanced to modulate PAs built around the CGH40025F with 70% average final stage efficiency.**

In February 2016 at Mobile World Congress, Eta Devices demonstrated what could be the highest efficiency GaN high power amplifier compliant to MC-GSM/LTE specifications. The linearity specification for MC-GSM is that distortion products must be lower than -60 dBc. According to Eta Devices, Cree GaN HEMTs can be used over a very wide range of drain bias voltages. They exploit this to achieve not only high efficiency at maximum average power, but also achieve high efficiency at back-off. Their demonstration uses Cree's high performance CGH40025F with high efficiency, high reliability and consistent performance.

Figure 10 shows measurements from Eta Devices' MWC 2016 demonstration. Eta Devices was able to demonstrate 70 percent average final stage efficiency for a fully modulated LTE carrier and >60 percent average final stage efficiency for MC-GSM transmissions. These efficiency numbers include the loss of the supply modulator.

Wolfspeed and Eta Devices have teamed together to design highly efficient amplifiers for base station applications that promise to greatly reduce power consumption, saving wireless communications providers millions in Op Ex for a greener future.

CONCLUSION

It was not long ago that 50 percent efficient power amplifiers were the best in the industry, but now, many manufacturers are obtaining 65 to 70 percent efficiency. GaN and advanced modulation and matching techniques are pushing efficiencies higher every year. ■

A Wideband High Efficiency Doherty Power Amplifier Based on Coupled Line Architecture

Guangping Xie , Zongxi Tang, Biao Zhang and Xin Cao
University of Electronic Science and Technology of China

A wideband high efficiency Doherty power amplifier (DPA) that works in the 1.85 to 2.4 GHz band (26 percent fractional bandwidth) employs two pairs of anti-coupled lines with stepped impedance resonators to replace the λ/4 transmission lines in a conventional DPA for harmonic suppression and phase compensation. Maximum output power is between 43.0 and 44.1 dBm. At 6 dB output power back-off (OPBO), the maximum drain efficiency (DE) is 61.3 percent, with gain higher than 12 dB. In the saturated output power region, the efficiency is between 67 and 76.6 percent with gain higher than 8 dB. Compared with a conventional DPA, the third-order intermodulation distortion (IMD3) is reduced by 22 dB while efficiency and gain performance are greatly improved.

In wireless communication basestations, Doherty power amplifiers[1] are widely used to provide high efficiency in the presence of modulated signals with high peak to average power ratios. The λ/4 transmission line in a conventional DPA is used mainly to perform impedance matching and provide phase delay compensation. The fractional bandwidth is typically narrow (usually less than 10 percent), because the λ/4 transmission line can achieve an optimum impedance transformation and phase compensation only at one frequency. This limits its application in multiband, multi-standard base stations. Moreover, the peaking amplifier in the DPA operates class C, and as a result, has relatively poor linearity.

The λ/4 transmission line in a conventional DPA also exhibits weak harmonic suppression. Some strategies to address this, like composite right/left-handed transmission lines (CRLH-TL), defected ground structures (DGS), analytical model simplification and harmonic tuning, have been successfully reported.[2–5] Fang and Quaglia[2] report a DPA with 18 percent fractional bandwidth; however, the DE and gain at 6 dB OPBO are only 36 percent and 6 dB, respectively. For comparable linearity, CRLH-TL and DGS were adopted with the standard DPA topology for a power-added efficiency (PAE) at 6 dB OPBO of about 20 percent.[3,4] Zhao et al.,[5] report on a similar case with measured results showing less obvious improvement in linearity by utilizing a simple analytical model. A 35 percent fractional bandwidth is reported by Bathich et al.,[6] by exploiting wideband filters; in this case, a standard topology is also adopted, but the Doherty behavior is not clearly demonstrated. Sarkeshi et al.,[7] employ frequency reconfigurable matching networks enabling a fractional bandwidth of about 20 percent; however, this requires an external control circuit.

In this work, a compact phase compensation architecture based on two pairs of anti-coupled lines loaded with stepped impedance resonators replaces the λ/4 transmission line in a conventional DPA. This structure performs impedance conversion, phase compensation, phase correction and harmonic suppression. At the same time, it provides an easy way to tune performance by adjusting the width and length of the stepped impedance resonators.

PHASE COMPENSATION NETWORK

Even/odd mode analysis was used to analyze the axially symmetric novel and compact DPA structure shown in ***Figure 1***. First analyzed is the two-port network in area 1. Z_{oe} and Z_{oo} represent the even mode and odd mode characteristic impedances of the parallel coupled line. $[Z_U]$, $[Z_D]$ and $[Z_T]$ represent the impedance matrices of the parallel coupled line, the low impedance line and the two-port network in area 1, respectively. The impedance matrix of the two-port network is given by[8,9]

$$[Z_T]=[Z_D]+[Z_U]=\begin{bmatrix} Z_{T11} & Z_{T12} \\ Z_{T21} & Z_{T22} \end{bmatrix} \quad (1)$$

where

$$Z_{T11}=j\left(Z_{oe}\tan\theta_e+Z_{oo}\tan\theta_o\right)/2-jZ_0\cot\left(\beta l_{om}\right)$$

$$Z_{T12}=j\left(Z_{oe}\tan\theta_e-Z_{oo}\tan\theta_o\right)/2-jZ_0\cot\left(\beta l_{om}\right)$$

$$Z_{T21}=j\left(Z_{oe}\tan\theta_e-Z_{oo}\tan\theta_o\right)/2-jZ_0\cot\left(\beta l_{om}\right)$$

$$Z_{T22}=j\left(Z_{oe}\tan\theta_e+Z_{oo}\tan\theta_o\right)/2-jZ_0\cot\left(\beta l_{om}\right)$$

θ_e and θ_o represent the even and odd mode electrical lengths, respectively. From the relation between the ABCD matrix and the impedance matrix,[9] we derive the ABCD matrix of the two-port network. The physical length of the microstrip curved line in area 2 is designated l and the ABCD matrix of the two-port network is designated $[M_H]$. These are given as follows,

$$[M_H]=\begin{matrix} A_H & B_H \\ C_H & D_H \end{matrix} \quad (2)$$

$$l=w_{in}+\pi\left(R_{inner}+R_{out}\right)/2 \quad (3)$$

where,

$$A_H=\frac{\cos(\beta l)\left[\cos(\beta l)Z_{T11}+jZ\ Y_0\sin(\beta l)\right]+jZ_0\sin(\beta l)\left[\cos(\beta l)+jY_0\sin(\beta l)Z_{T22}\right]}{Z_{T21}}$$

$$B_H=\frac{\cos(\beta l)\left[jZ_0\sin(\beta l)Z_{T11}+Z\ \cos(\beta l)\right]+jZ_0\sin(\beta l)\left[jZ_0\sin(\beta l)+\cos(\beta l)Z_{T22}\right]}{Z_{T21}}$$

$$C_H=\frac{jY_0\sin(\beta l)\left[\cos(\beta l)Z_{T11}+jZ\ Y_0\sin(\beta l)\right]+\cos(\beta l)\left[\cos(\beta l)+jY_0\sin(\beta l)Z_{T22}\right]}{Z_{T21}}$$

$$D_H=\frac{jY_0\sin(\beta l)\left[jZ_0\sin(\beta l)Z_{T11}+Z\ \cos(\beta l)\right]+\cos(\beta l)\left[jZ_0\sin(\beta l)+\cos(\beta l)Z_{T22}\right]}{Z_{T21}}$$

and then $Z=Z_{T11}Z_{T22}-Z_{T12}Z_{T21}$

The networks in areas 2 and 3 are symmetric and have a parallel relationship. $[M_F]$ represents the ABCD matrix of the two-port network that consists of the structures in areas 2 and 3. By analyzing the relation between voltage and current of the two-port networks of areas 2 and 3, $[M_F]$ is given as follows,

$$[M_F]\begin{bmatrix} A_H & B_H/2 \\ 2C_H & D_H \end{bmatrix} \quad (4)$$

A_H, B_H, C_H and D_H are defined in Equation 2.

The input microstrip line in area 5, the output microstrip line in area 4 and the parallel network of areas 2 and 3 have a cascade relationship. With $[M_G]$ representing the ABCD matrix of the entire structure and $[M_K]$ representing the input microstrip line in area 5, $[M_G]$ is given as

$$[M_G]=[M_K][M_F][M_K]=\begin{bmatrix} A_G & B_G \\ C_G & D_G \end{bmatrix} \quad (5)$$

From the relationship between the ABCD matrix and the scattering matrix,[9] the scattering parameters of the structure are

$$S_{21}=2/A_G+B_G/Z_0+C_GZ_0+D_G=\left|S_{21}\right|e^{j\varphi_{21}} \quad (6)$$

$$S_{11}=\left(A_G+B_G/Z_0-C_GZ_0-D_G\right)/\left(A_G+B_G/Z_0+C_GZ_0+D_G\right)=\left|S_{11}\right|e^{j\varphi_{11}} \quad (7)$$

$$Z_{21}=1/C_G=\left|Z_{21}\right|e^{j\psi_{21}} \quad (8)$$

φ_{21}, φ_{11} and ψ_{21} are the phase of S_{21}, S_{11} and Z_{21}, respectively. A_G, B_G, C_G and D_G are given in Equation 5. Using design specifications for $|S_{21}|$, $|S_{11}|$, $|Z_{21}|$ and φ_{21} and Equa-

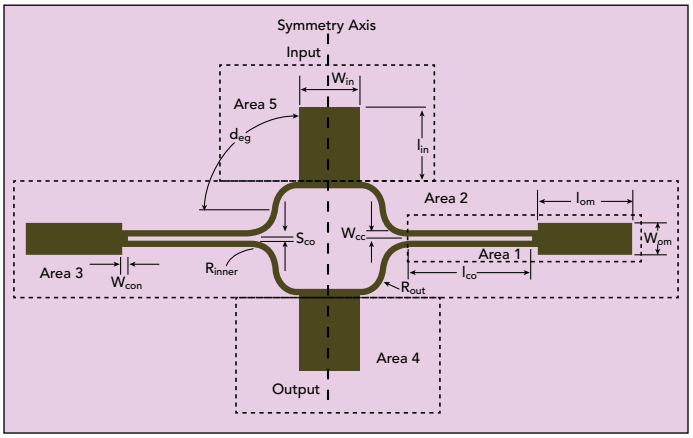

▲ **Fig. 1 Phase compensation structure for the Doherty power amplifier.**

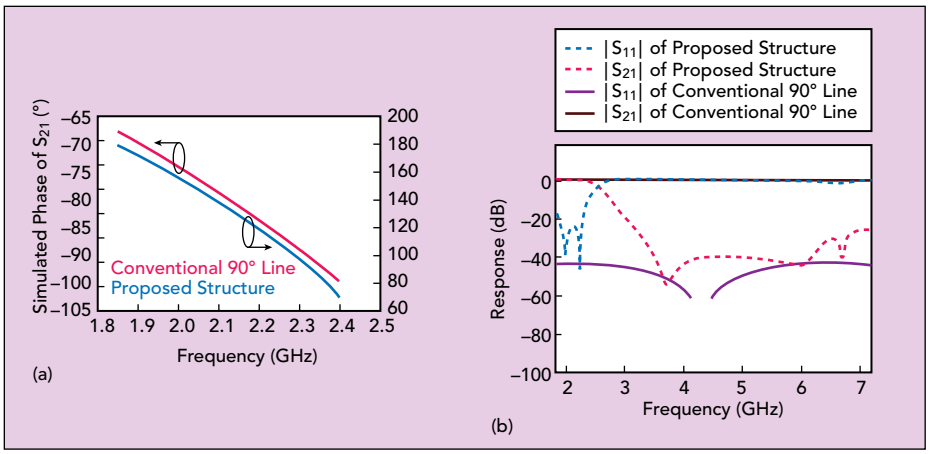

TABLE 1

Z_{21} OF THE PROPOSED STRUCTURE

f (GHz)	$\|Z_{21}\|$	Phase (°)
2.10	62.42	91.89
2.15	55.07	91.38
2.20	54.76	90.84
2.25	53.57	90.29
2.30	55.65	89.62
2.35	61.66	88.67

Fig. 2 Simulated performance of the phase compensation structure vs. a conventional 90° line: ∠ S_{21} (a), $|S_{11}|$ and $|S_{22}|$ (b).

tions 6–8, a compact phase compensation architecture based on two pairs of anti-coupled lines with stepped impedance resonators is implemented.

Figure 2 shows its simulated performance. The simulated transmission phase of the structure is shown in Figure 2a, while the magnitude of the S-parameters is shown in Figure 2b. Figure 2b shows that the conventional λ/4 transmission line provides almost 0 dB harmonic suppression, while second harmonic suppression is better than 40 dB and third harmonic suppression is about 30 dB in the new structure. ***Table 1*** shows the characteristic impedance of the structure, which is around 50 Ω. A compact structure implemented by capacitor-loaded coupled lines is reported by Li et al.,[8] but its second and third harmonic suppression is only about 20 dB. Zhang et al.,[10] report on a structure consisting of a pair of anti-coupled lines short circuited by a low impedance line; however, second and third harmonic suppression are also limited to around 20 dB.

REALIZATION AND CHARACTERIZATION

To verify this design, a DPA operating over a 1.85 to 2.4 GHz band was realized. It is fabricated on a Taconic substrate with copper metallization (RF35 with a relative dielectric constant ε_r = 3.5, substrate height h = 0.508 mm, metal thickness t = 0.035 mm and loss tangent tan δ = 0.0018). The main and peaking power amplifiers are implemented with Cree CGH40010F GaN HEMTs.

Figure 3 shows the block diagram and photo of the implemented DPA, respectively. A Wilkinson power divider splits the input power equally. The location of the phase compensation structure is indicated in Figure 3a. The dimensions of the DPA are approximately 1.5 λg × 1 λg, where λg is the guide wavelength at center frequency f_0 = 2.125 GHz.

Measurements were taken in 50 MHz steps with single-tone CW excitation. The main PA operates class A/B with V_{DS} = 28 V and V_{GS} = -2.5 V (I_d = 210 mA). The peaking PA operates class C with V_{DS} = 28 V and V_{GS} = -3.7 V. Measured and simulated power gain as a function of output power are shown in ***Figure 4***. Differences between measurement and simulation at low and moderate output power are attributed to simplifying assumptions used in the model for the PA output load impedance. Saturated gain is higher than 8 dB, as shown in both measurement and simulation. Figure 4b shows measured and simulated gain as a function of frequency at 6 dB OPBO and win saturation. Gain at 6 dB OPBO is higher than 12 dB in the 1.85 to 2.4 GHz band. Gain flatness is similar at 6 dB OPBO or when saturated. ***Figure 5a*** shows the measured and simulated output power as a function of input power at 1.85, 2.1 and 2.4 GHz. Saturated output power over frequency is shown in ***Figure 5b***; the saturated power is between 43 and 44.1 dBm.

The DE at saturated output power and 6 dB OPBO as a function of frequency and output power are shown in ***Figures 6a*** and ***6b***, respectively. The DE at saturation is between 67 and 76.6 percent, and the drain efficiency at 6 dB OPBO is between 35 and 61.3 percent. Measured and simulated DE at saturation are comparable; however, the drain efficiency at 6 dB OPBO shows some differences from the simulated results. This is due mainly to the influence of fabrication tolerances.

Figure 7 shows the measured IMD3 of the DPA based on this work versus a conventional DPA, using two tones spaced 6 MHz apart, at 1.85, 1.90, 2.08 and 2.15 GHz. The IMD3 is improved by about 22 dB at high-power compared to the conventional DPA. In the region where output

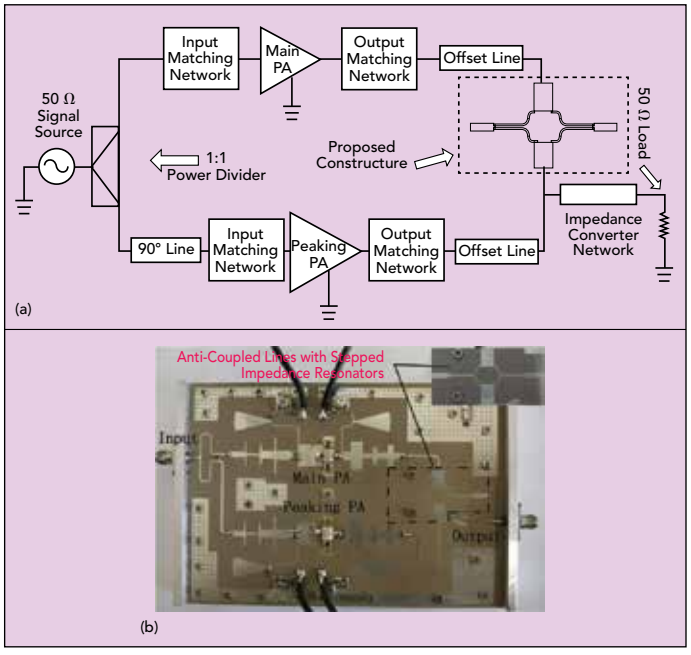

Fig. 3 Block diagram (a) and fabricated (b) DPA.

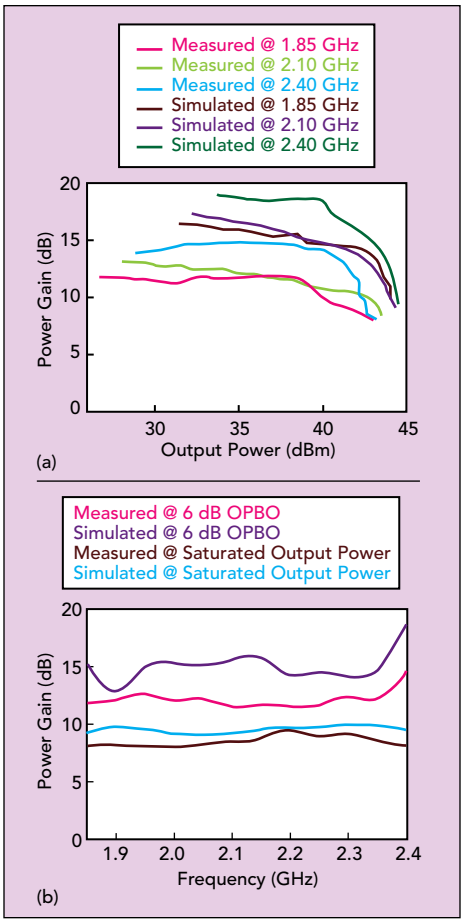

Fig. 4 Measured and simulated power gain vs. output power (a) and frequency, at 6 dB OPBO and saturation (b).

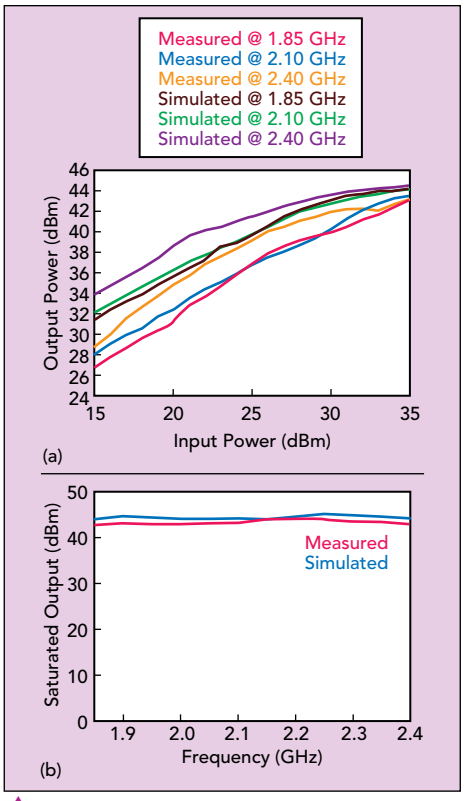

Fig. 5 Measured and simulated output power vs. input power (a) and saturated output power vs. frequency (b).

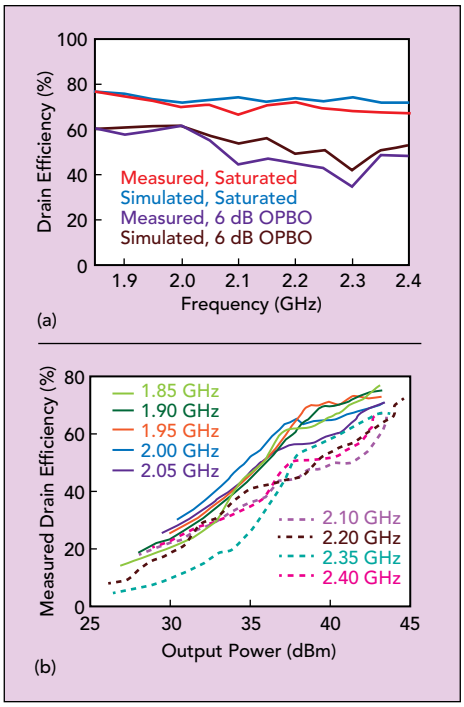

Fig. 6 Measured and simulated drain efficiency vs. frequency at 6 dB OPBO and saturation (a); measured drain efficiency vs. output power vs. frequency (b).

power is higher than 30 dBm, the best IMD3 is -44 dBc at 2.08 GHz. IMD3 performance is improved across the board. Note the rise in IMD3 as the output power is increased above 38 dBm. This is because the peaking amplifier is completely turned on, generating more third-order intermodulation.

DPA performance from this work is compared with other reported results in ***Table 2***.[4,11-13] Several DPAs with fractional bandwidths higher than 30 percent are shown, but their saturated efficiencies and efficiencies at 6 dB OPBO are lower. The DPA described by Sun and Jansen[12] achieves a bandwidth higher than 30 percent, but its best IMD3 is only -35 dBc at high-power.

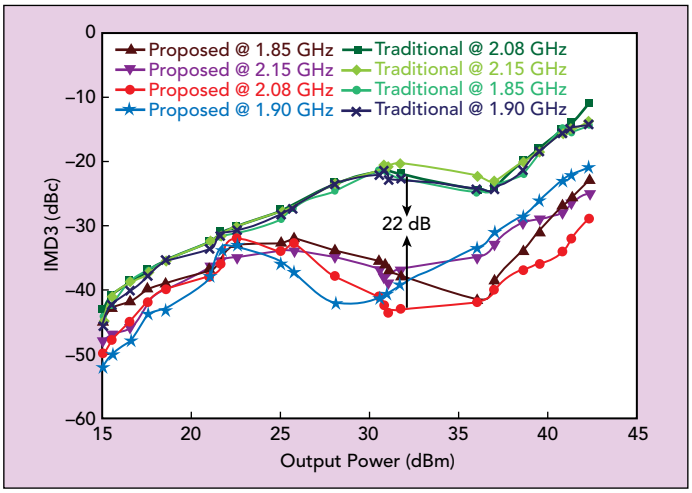

Fig. 7 Measured IMD3 performance vs. output power, comparing the coupled line design with a conventional Doherty.

CONCLUSION

A compact phase compensation architecture based on two pairs of anti-coupled lines loaded with stepped impedance resonators replaces the λ/4 transmission line in a conventional DPA. Compared to a conventional DPA, this design demonstrates an improvement in efficiency, gain and IMD3.■

References

1. W. H. Doherty, "A New High Efficiency Power Amplifier for Modulated Waves," *Proceedings of the Institute of Radio Engineers*, Vol. 24, No. 9, September 1936, pp. 1163–1182.
2. J. M. Rubio, J. Fang, V. Camarchia, R. Quaglia, M. Pirola and G. Ghione, "3 to 3.6 GHz Wideband GaN Doherty Power Amplifier Exploiting Output Compensation Stages," *IEEE Transactions on Microwave Theory and Techniques*, Vol. 60, No. 8, August 2012, pp. 2543-2548.
3. Y. C. Jeong, S. G. Jeong, J. S. Lim and S. Nam, "A New Method to Suppress Harmonics Using Bias Line Combined by Defected Ground Structure in Power Amplifiers," *IEEE Microwave and Wireless Components Letters*, Vol.13, No.12, December 2003, pp. 538-540.
4. S. H. Ji, S. K. Eun, C. S. Cho, J. W. Lee and J. Kim, "Linearity Improved Doherty Power Amplifier Using Composite Right/Left-Handed Transmission Lines," *IEEE Microwave and Wireless Components Letters*, Vol. 18, No. 8, December 2008, pp. 533–535.
5. Y. Zhao, A. G. Metzger, P. J. Zampardi, M. Iwamoto and P. M. Asbeck, "Linearity Improvement of HBT-Based Doherty Power Amplifiers Based on

TABLE 2

COMPARISON OF REPORTED WIDEBAND DPAS

References	4	11	12 (Version 1)	13	This Work
Frequency (GHz)	3 to 3.6	1.7 to 2.4	2.2 to 3.0	1.63 to 1.98	1.85 to 2.40
P_{sat} (dBm)	44 to 43	41.5 to 34.5	41.8 to 40.2	34 to 31	44.1 to 43.0
Saturated DE (%)	65 to 56	53 to 72	68 to 52	60 to 44 (PAE)	76.65 to 67
DE @ 6 dB OPBO (%)	54 to 38	59 to 43	53 to 30	49 to 20 (PAE)	61.3 to 35
Gain (dB)	11.2 to 6	10.1 to 8.6	8.7 to 5.5	17 to 6	14.8 to 8.0
Max IMD3 (dBc)	–	–	–35 (IMD3 Upper)	–	–44.0
Type	GaN HEMT	GaN HEMT	GaN HEMT	GaN HEMT	GaN HEMT

a Simple Analytical Model," *IEEE Transactions on Microwave Theory and Techniques*, Vol. 54, No. 12, December 2006, pp. 4479–4488.

6. K. Bathich, A. Markos and G. Boeck, "A Wideband GaN Doherty Amplifier With 35 Percent Fractional Bandwidth," *Proceedings of the European Microwave Conference*, September 2010, pp. 1006-1009.
7. M. Sarkeshi, O. B. Leong, and A. van Roermund, "A Novel Doherty Amplifier for Enhanced Load Modulation and Higher Bandwidth," *IEEE MTT-S International Microwave Symposium Digest*, June 2008, pp. 763–766.
8. R. Li, D. I. Kim and C. M. Choi, "Compact Structure With Three Attenuation Poles for Improving Stopband Characteristics," *IEEE Microwave and Wireless Components Letters*, Vol. 16, No. 12, December 2006, pp. 663–665.
9. D. M. Pozar, *Microwave Engineering*, 3rd ed., Wiley, N.Y., 2005.
10. J. Zang, L. Li, J. Gu and X. Sun,"Compact and Harmonic Suppression Wilkinson Power Divider With Short Circuit Anti-Coupled Line" *IEEE Microwave and Wireless Components Letters*, Vol. 17, No. 9, September 2007, pp. 661-663.
11. L. Piazzon, R. Giofrè, P. Colantonio and F. Giannini, "A Wideband Doherty Architecture With 36 Percent of Fractional Bandwidth," *IEEE Microwave and Wireless Components Letters*, Vol. 23, No. 11, November 2013, pp. 626-628.
12. G. Sun and R. H. Jansen, "Broadband Doherty Power Amplifier Via Real Frequency Technique," *IEEE Transactions on Microwave Theory and Techniques*, Vol. 60, No. 1, January 2012, pp. 99-111.
13. S. Watanabe, Y. Takayama, R. Ishikawa and K. Honjo, "Miniature Broadband Doherty Power Amplifier With a Series-Connected Load," *IEEE Transactions on Microwave Theory and Techniques*, Vol. 63, No. 2, February 2015, pp. 572-579.